RADIO-OVER-FIBER SYSTEM MODELING WITH TURBO CODED OFDM FOR IMPROVED BIT ERROR RATE

by

Saeed Shams

2011-NUST-MS PhD-Elec(Com-N)-13

Submitted to the Department of Electronic and Power Engineering in fulfillment of the requirements for the degree of

MASTER OF SCIENCE
in
ELECTRICAL ENGINEERING
Specialization in Communication

Supervisor

Dr. Khawaja Bilal Ahmed Mahmood

Co-Supervisor

Dr. Sameer Hashmat Qazi

Pakistan Navy Engineering College, Karachi

National University of Sciences & Technology

February 2015

بسم الله الرحمن الرحيم

Acknowledgments

Abstract

Radio-over-Fiber (RoF) systems are employed to carry wireless signals through optical fiber. Light signals are the data carriers in an optical medium.

The need for communications system architecture that is low cost and far reached too; is inevitable for under-developed countries like Pakistan. RoF is an established technology mainly due to the operational expenditures (OPEX) cost cuts it can provide and also for its wide range of applications.

With the increasing number of users for high speed information exchange, the data transmission now requires even more integrity and sustainability which can be incorporated by the use of this technology.

RoF systems use the optical communication for its efficient, high capacity and data-rate carrying property. To economize the frequency spectrum, and provide integrity of data against dispersive channels, orthogonal frequency division multiplexing (OFDM) is considered the most widespread scheme for wired and wireless technologies equally.

The aim of this thesis is to employ low cost RoF transmission technique and to provide a method for improving the bit error rate (BER) of the optically transmitted data with the help of increased data redundancy by employing turbo codes in conjunction with OFDM, which can also be referred to as Turbo Coded OFDM.

For the proposed method, extensive modeling and simulations were done and the results were compiled by performing the simulations for different parameter variations. The radio signal transmission was carried out through optical fiber after OFDM modulation and received at the photodiode before getting demodulated and decoded.

The simulation platform was made by the integration of Matlab and the optical simulator OptiSystem. The data transmission/reception link was simulated in OptiSystem while the coding/decoding was carried out in Matlab.

Table of Contents

List of Figures

List of Tables

1. Introduction

1.1   Age of Information

Ever since civilization has existed, mankind's learning process has continued with varying magnitudes. The extent of communication or the amount of information exchange has mainly defined the degree by which the development of noesis (the psychological result of perception and learning and reasoning) and lifestyle for humans has occurred.

In today's world, this information exchange has essentially become the source of life for almost all the domains and aspects relating to everyday life, as Internet has joined together leisure, work, politics and things that we use; to the network. At the same time with continuous expansion going on and with an ever increasing exposure, it also has become a benchmark of quality and success for most developed countries.

1.2   Growing Wireless Access technologies

With the rapid development of the next generation of mobile communication technology, the past few years have witnessed a growing demand for broadband internet access on the move[1], with gigabit per second communication in fact becoming the protocol for data transmission[2]. Last year's IP traffic amounted to roughly 41 thousand peta-byte (PB) per month, with annual growth rate predictions of 20% for Internet, and an exploding 62% annual growth for Mobile data [3].

Due to the demand for greater bandwidth and higher data-rates, the consumer majority is approaching newer and faster technologies available; forcing the operators to evolve their network architecture. Although 2G and 3G networks have not yet saturated globally, with Pakistan launching 3G only a few months ago, the constant transition along with 4G deployment is becoming a worldwide phenomenon. The huge 80% of the total mobile subscriptions are predicted for mobile broadband in the next five years [4, 5].
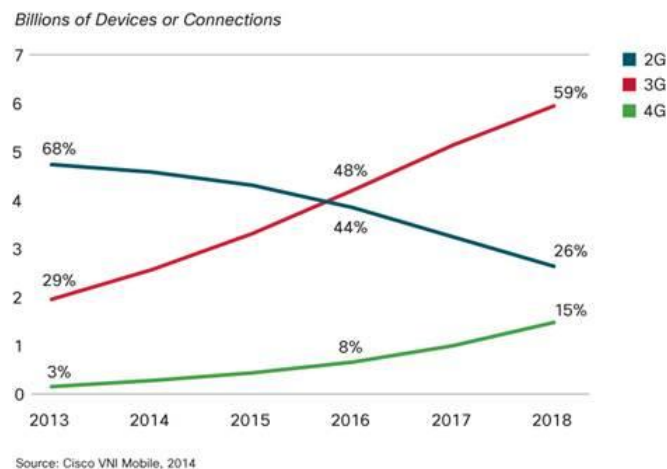
Figure 1.1: Mobile Devices and Connections around the world by 2G, 3G, and 4G [4]

Although new networks being deployed still set their platform on the industry standards defined by the 3rd Generation Partnership Project (3GPP)[6] for Long-Term Evolution (LTE); which promises a sizeable capacity increment than the vastly deployed 3rd Generation (3G) networks[2], but operators are already putting to test the true 4G networks for the ever growing user base [6].

1.3   Wireless Communication Systems

The air is the medium for communication in wireless networks, with applicability ranging from a simple remote controller for an appliance to complex military applications on the field. The mobility, simplicity and the constant maturity of this mode of communication has made it the popular choice for many[7].

Wireless technologies are classified mainly by their coverage areas and the bandwidth and data-rates they could provide. Some of the technologies are briefly described with example while their respective coverage areas and data-rates are provided in Figure 1.2.

- **Mobile communication**

  2G e.g. GSM and 3G e.g. universal mobile telecommunication system (UMTS) systems have cells spanning several kilometers, but have data-rates limited to less than 2 Mbps.

- **Wireless Metropolitan Area Network WMAN**

  They provide high data-rates coupled with extended coverage, e.g. IEEE 802.16 standard.

- **Wireless Personal Area Network WPAN**

  The cell sizes in wireless personal area networks (WPANs) are usually a few meters (pico-cell), with transmission rates reaching nearly thousands of Mbps. e.g. IEEE 802.15c standard.
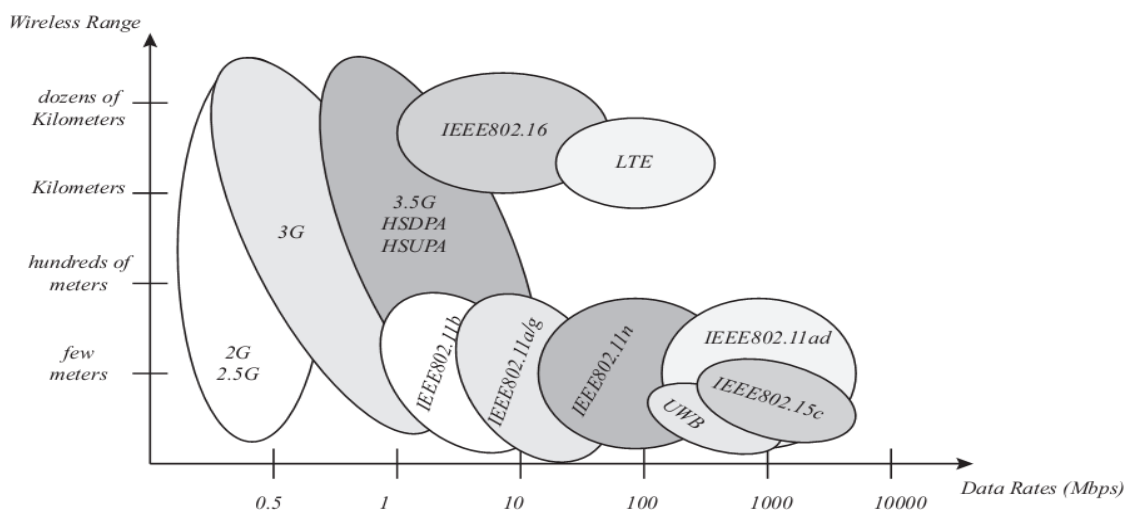
Figure 1.2: Data-rates and range requirements for wireless standards and applications [8]

- **Wireless Local Area Network WLAN**

The most commonly used standards for wireless internet connectivity around the world, these standards are developing briskly with newer high data-rate standards being tested. e.g. IEEE 802.11 standard.

With the growing user base, the sharing of the wireless medium is one of the biggest challenges faced by the providers[9].

1.3.1 Capacity and Coverage

The different standards and their data-rates along with their respective coverage spans are brought together in Figure 1.2. There is a trade-off between capacity and coverage; since mobile communication systems try to increase capacity, and wireless data systems try to increase coverage, consequently they will both move towards convergence [10].

The possible capacity increment procedures have had their own drawbacks. Employing low carrier frequencies in general provide with low cost radio front-end in base station (BS) and mobile unit/wireless terminal unit (MU/WTU), a low bandwidth, but a larger coverage area. At the same time large cells can be less efficient as many MU/WTU share a single cell. Lower power can be utilized for creating smaller cells, but it would require more BS's and extensive feeders for coverage. High carrier frequencies provide relief from the congested ISM (industrial, scientific and medical) bands and offer higher bandwidth [11] but increase radio front end costs and a decreased cell size [6, 10].

1.4 Network Simplification

There is a need for special techniques to provide the ever increasing data transmission and capacity; an architecture or a structure that might cater to the new and the coming generations' standards [1], on an equality basis. This has prompted research for a simplified yet robust model for the wireless network. As the newer standards of wireless communication are using higher frequency bands[11], the enhancement of system and link capacity requires an infrastructure that collects and distributes the radio signals from different antennas, commonly known as distributed antenna system (DAS), shown in Figure 1.3.
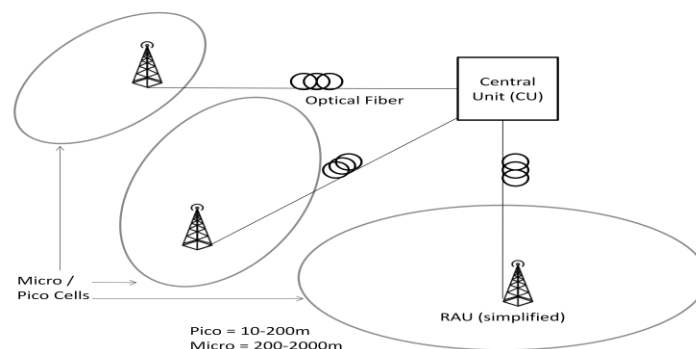
Figure 1.3: A RoF link scenario with DAS for mobile and wireless communication using the micro/pico cells concept

With optical fiber's bandwidth and low-loss features, the RoF technology provides the necessary simplification of the network by centralizing the radio signal processing at the central unit (CU) while remote antenna unit (RAU) simply radiates the signal received through optical fiber [6, 10].

1.5 Optical Communication Systems

Optical communication became possible after the advent of Lasers in the 1960's [6], and in around a span of ten years or more the first optical fiber was deployed which revolutionized the whole telecommunication domain with its capabilities and dependability. The optical fiber provided the much needed low loss, high capacity and isolation from exterior interferences to the long distance communication. Optical fiber transmission has developed during the last 30 years catering for different types of transmission including distant, high-speed, under-water as well as for local area networks [6].

A simple optical communication system consists of a light source acting as the transmitter, an optical fiber cable for carrying the data, an optional optical amplifier for longer distances when signals get degraded, and a detector that receives the data transmitted as shown in Figure 1.4.
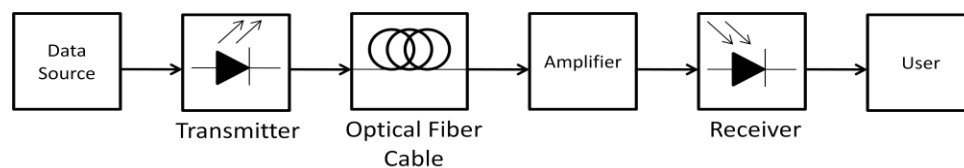
Figure 1.4: A simple optical fiber link

The source delivers the data to the transmitter; which is coupled to the optical fiber, modulates the data on an optical carrier (light pulses) which is transmitted through the optical fiber later to be received by the photo-detector and to be converted back to its original form.

Exchanging of data and conveyance to broadband wired and wireless networks can be done through different mediums, like coaxial cables and copper twisted pairs, but optical fiber is the preferred medium [8].

1.6 Radio-over-Fiber (RoF) system for communication

The radio-over-fiber (RoF) technology is the unification of wireless and optical platforms and has been considered throughout the years as a guaranteeing model for broadband communications, also because it can ideally transport and distribute several wireless signals and standards to the BS antennas using the same medium in a transparent manner [6, 8, 10].

The basic RoF link consists of the hardware components required to convert and modulate a wireless signal on an optical carrier, also it contains the optical fiber link for transmission and the receiver part to detect and recover the transmitted signal. A common RoF link simplifies the BS by removing the data processing blocks, focusing the computing load at a central station as shown in Figure 1.5.
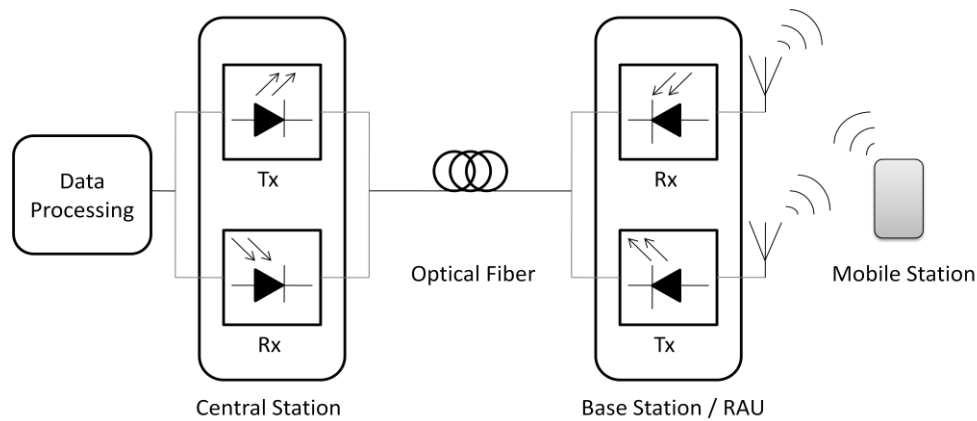
Figure 1.5: Radio over Fiber System illustration[10]

To provide the RoF system with an efficient utilization of the frequency spectrum while keeping the data integrity, the orthogonal frequency division multiplexing (OFDM) was considered. With its robustness against dispersive channels and the capability of transporting multiple channels simultaneously made OFDM the modulation scheme for high data-rate wired and wireless standards not only for the current but also for the next generation technologies [8].

1.7   Problem Statement

As emphasized above, increased demand for capacity by high bit rate traffic called for a distributed yet simplified structure allowing the different standards to utilize a common platform. Radio-over-Fiber technology was considered for the future of high speed networks, but the costs and losses related to optical communications make it a domain for constant improvement.

To provide a cost-effective solution for the growing wireless networks in developing countries and in Pakistan, a simulated model of the radio-over-fiber system with low cost lasers and simple intensity modulation-direct detection techniques was carried out in the study. OFDM can provide high spectral efficiency therefore it is considered an integral part of wireless communication system and is tested along with the performance of Turbo codes and bit interleaver technologies, proposed to effectively mitigate unbalanced error distribution.

1.8   Objectives

The few objectives of this study are to:

- Employ and investigate an effectively operational model of the RoF link while analyzing the effects of various parameters on the RoF link.
- Implementation of turbo coding and decoding would be carried out in the Matlab and Simulink environment while the integration of Matlab with the optical simulator OptiSystem for provision of coded data to the link is going to be an integral part of the study.
- Evaluating the performance of the system along with bit error rate (BER) readings and compilation of the results and analysis for a possible publication are also a part of the study objectives.

1.9   Thesis Organization

The chapters to follow in this thesis are assembled as described,

Chapter 2 defines the RoF technology along with the transmission and modulation concepts and link configurations of the optical communication system, and the limitations and applications of RoF technology.

Chapter 3 presents the theoretical description of the OFDM scheme with the modulation techniques that are employed and the complete system description as well as the importance of coding in OFDM.

Chapter 4 describes the concept of turbo codes and their affectivity along with the configurations and the individual model for the simulations.

Chapter 5 puts forward the simulation model and the analysis of the complete system modeled together with the plotting and results collected.

Chapter 6 concludes the whole study with a summarized description and also provides suggestions for future works and adjustments related to the system presented.

2 Radio-over-Fiber (RoF)

2.1 Introduction

The recent popularity of high capacity data access and sharing on the internet; including videos and images have predicted that the content delivery networks would be carrying more than half of the internet traffic in the next five years. Also with the broadband speeds growing and the number of users, the wireless and mobile devices would surpass the wired devices with respect to the internet traffic in the coming years [3].

The RoF system provides a viable solution to the growing demand for bandwidth and speed by providing a system which provides a transparent interconnection of a base station with its transmission and receiving antennas by means of an optical network, therefore increasing the bandwidth carrying capacity to and from the central station terminal to the RAU and allowing the data processing capability to be shared by RAUs from a central station.

2.2 RoF System Concept

The RoF system's fundamental function is the transmission of analog wireless signals through an optical fiber by transposing wireless signals on to the optical carrier, that is the processed digital baseband data is modulated onto an analog waveform and, this analog waveform at radio frequency (RF) or at an intermediate frequency (IF) is used to modulate the optical source. It does not matter if the baseband modulation format is a digital format (such as BPSK, QAM), indicating a set of discrete available amplitudes, that is the reason it is referred to as analog modulation [12].

The electrical to optical conversion of the radio signal is achieved by the modulation of the light source, usually a laser diode. The light pulses after travelling the optical channel are converted back to the electrical domain by the photo-detector, usually a photodiode.

In a RoF system downlink the whole process of preparation of data for transmission on an optical fiber is carried out in the central station, while the detection of data and transferring it to the antennas is carried out at the BS. The uplink is the reverse of the downlink process as shown in Figure 2.1. Thus, the simplification of the RAU is achieved with the system intelligence focusing in on the center, and allowing for low cost sharing, easy future upgrading of the central resource and system maintenance [13].
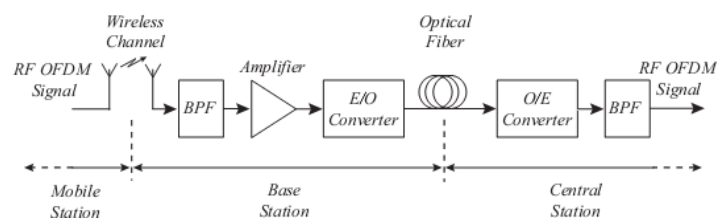
Figure 2.1: A RoF system model for uplink [8]

Mostly RoF systems communicate the radio signals in the analog modulation form as discussed above, except for one scheme that brings us to the classification of the RoF systems according to the transmission schemes to be discussed in the following section.

2.3 Radio-over-Fiber Systems Classification

Different RoF systems can be described by the following classifications.

2.3.1 Frequency Ranges

The conventional principle in a RoF transmission is to convey an analog signal by modulating light to be transmitted through fiber. Depending on the transmission frequencies; Baseband-over-fiber, IF-over-fiber and RF-over-Fiber are the typical methods of transmission [12, 13]; with digitized IF-over-fiber being the latest scheme to be employed [6].

So, the most common type of digital optical communication is the baseband over fiber [14] in which a radio signal is transposed into baseband with a center frequency of zero before it modulates the optical carrier, but due to the signal processing requirements at the BS, a less complex option is preferred [12].

The IF-over-fiber scheme down converts the RF signal before modulation of the optical source and up converts it after detection with its advantages being suitable for high operational frequency systems. The RF-over-Fiber is the simplest scheme for the transport in which a radio signal is transposed to an optical carrier without changing its frequency as shown in Figure 2.2, this scheme eliminates all up/down conversions at the BS [8].
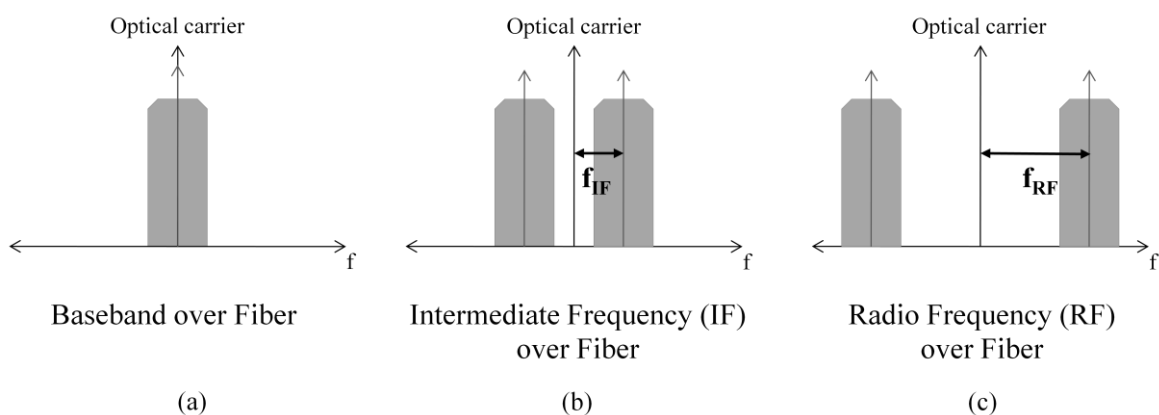
Figure 2.2: (a) Baseband (b) Intermediate frequency (f_{IF}) and (c) Radio frequency (f_{RF}) transmission schemes for RoF systems [15]

The digitized IF-over-Fiber scheme is adopted for WiMAX and 3GPP/LTE wireless systems in the industry standards; its function is to convert the radio signal to IF or RF, and then change the radio signal

waveform into digital format before modulating the optical source, this approach brings certain immunity to the signal to noise degradation present in the analog IF/RF-over-Fiber schemes [6].

2.3.2   Modulation Types

The RoF systems transmit radio signals through the optical fiber by modulating the light pulses, this phenomenon is called the intensity modulation (IM) where intensity of the optical signal being transmitted is proportional to the modulating signal, and the modulation can be recovered by direct detection (DD) from photodiode. The intensity modulation direct detection (IM-DD) technique is covered by the RF-over-Fiber category as well and is mostly the universal choice for RoF applications [10, 16].

The two basic modulation schemes used in the IM-DD technique are direct modulation and external modulation. In direct modulation the radio signal directly modulates the laser's drive current if the signal is within laser's modulation bandwidth, while in external modulation the bandwidth requirement is overcome by the electro-optic modulator (EOM) which gives large bandwidth and the laser provides light signal by operating in continuous wave (CW) mode. The constant power from laser is then modulated by applying modulation signal to the electrodes of the external modulator, typically a mach-zehnder modulator (MZM) [16]. Both the schemes for intensity modulation along with the electro-optical conversions (in dashed boxes) are shown in Figure 2.3.

(a) Direct Modulation

(b) External Modulation
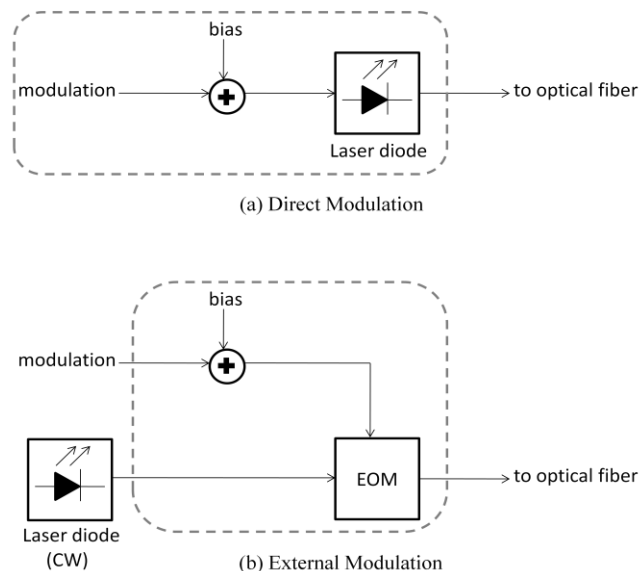
Figure 2.3: Basic intensity modulation (IM) techniques (a) Direct (b) External modulation with E/O conversion [12]

2.3.3   Fiber Types

The optical fibers are typically composed of a core and a cladding with the latter's refractive index lower than core which provide total internal reflection for the light to travel. The differences between the two

main categories of optical fibers; single-mode fiber (SMF) and multi-mode fiber (MMF) are the core and cladding radii, with SMF having a core radius of 8-10 um matching a light's wavelength, the MMF which guides multiple modes has a core radius of 50-62.5 um [12].

RoF systems have been deployed both with the SMF and MMF networks for long and short reach applications respectively [17]. For its easier handling and availability of low cost components and maintenance the MMF is used in in-house networks while SMF, for its high performance in access networks and long distance communications, is used for dealing with modal dispersion effects present in MMF but other dispersion effects occur like chromatic dispersion which causes signals at different optical frequencies (ν) to propagate at different speeds due to the change in refractive index with ν. The loss caused by fiber's attenuation depends on the wavelength; its viable bound was found at 0.2 dB/km at a wavelength of 1.55 um [12]. Transporting broadband microwave signals with RoF innovations can be done for SMF and MMF based systems with better efficiency by routing and dispersion control schemes [17].

2.4 Optical Transmitters

The RF signals transmission over fiber are less complex to implement using the (IM/DD) techniques, but for multi-GHz signals it might require very high frequency transmitters and receivers. As discussed before, intensity modulation of an optical carrier can be done by two methods. First is by direct RF modulation of a laser and the second is to modulate the CW optical carrier via an external modulator, like a MZM. The similarity in both the cases is the modulating analog RF signal. If data is carried by the RF signal, then the photocurrent amplitude after detection is proportional to the transmitted RF signal which can ideally preserve the modulation format.

A comparative analysis of direct and external modulation techniques reveals that Direct modulation of the laser is one of the least expensive and most simple of both schemes. However, one factor to note is the usable bandwidth ranges from DC to the laser relaxation frequency, which is nearly a few tens of GHz for high performance lasers [18].
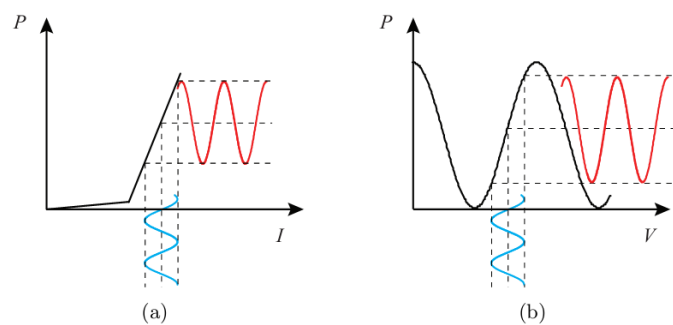
Figure 2.4: Schematic showing the relation between output optical power and RF signal amplitude for (a)Laser, (b)MZM [8]

The (nonlinear) relation between the output optical power and the drive current or voltage, for the laser and MZM, and their response to a sine wave signal is shown in Figure 2.4. in a generic form.

Both the laser and external modulators like MZM are nonlinear devices, but lasers are frequency dependent while MZM is frequency independent. The frequency dependence of the laser devices are further defined with simulative analysis in the following sections.

2.4.1   Rate Equations Laser (RE-Laser)

The Optisystem's RE-Laser component utilizes the rate equations to simulate the modulation dynamics of a laser which are modeled by the coupled rate equations which describe the relation between the carrier density, photon density, and optical phase [16].

The characteristic which defines an electro-optic converter is the light-current (LI) curve which exhibits the available power for a specific applied current. The default physical parameters of the component define a threshold current value of 33.45mA. The LI curve for a RE-laser is obtained by implementing the following layout in Optisystem..
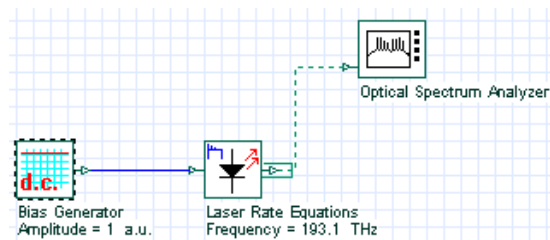
Figure 2.5: RE Laser layout for LI curve calculations

The figure shows the values used for the different components and the global parameters are kept at default values for the readings, with bitrate set at 10 Gbps and sequence length of 128 with 64 samples per bit. The LI curve was plotted with the readings and is shown in Figure 2.6.
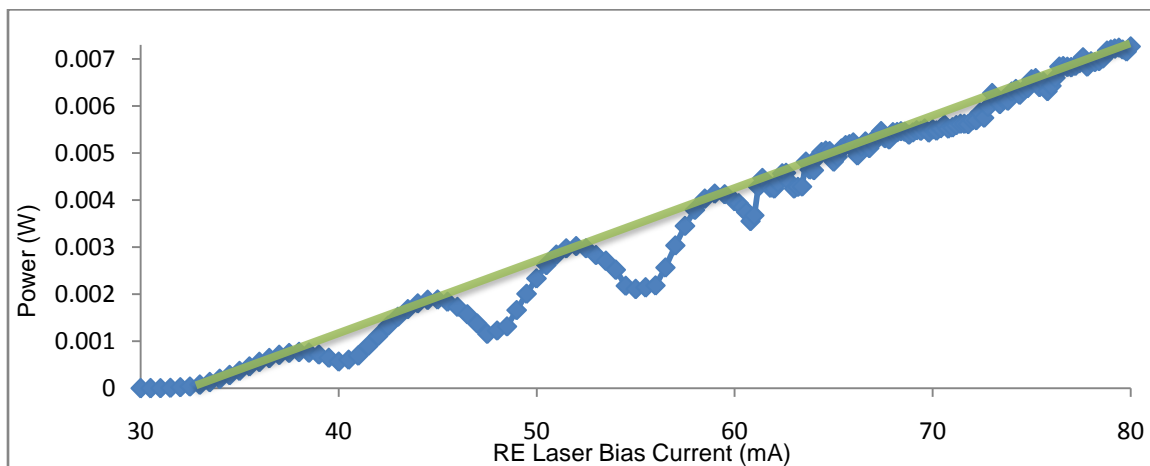
Figure 2.6: RE Laser LI curve plotted with readings obtained from Optisystem simulations

The RE-laser's input bias current parameter was varied between 30 to 80 mA with the corresponding reading of the received power at photodiode recorded. As we can see the curve is almost linear after the threshold current value is crossed.

Link gains for the various current biases, current amplitudes and carrier frequencies are analyzed next to depict the laser performance. In the paragraphs ahead, starting with the plot for input bias current readings against the link gain, the following layout is used for the calculations.
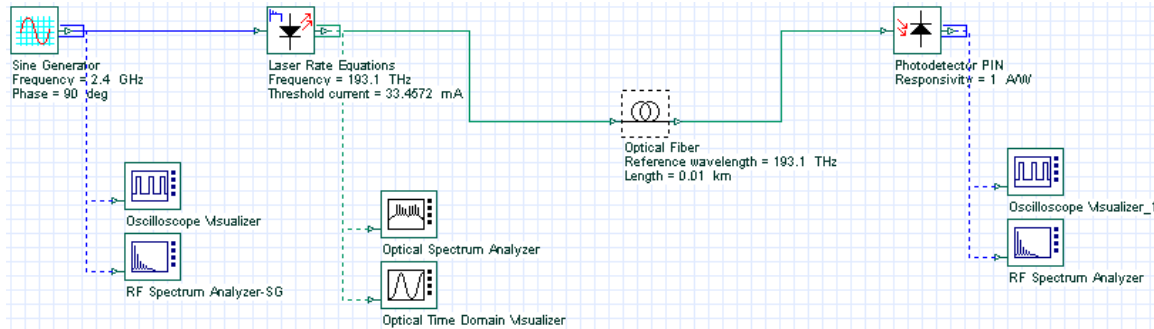
Figure 2.7: Layout for the RE-Laser operating characteristics calculations

The global parameters are set to default with parameter values for different components being configured as exhibited in the layout shown above.

The link gain [15] was calculated from the difference of the RF signal output power and the input power, both expressed in dBm.

$$G_i = S_{out} - S_{in} \tag{2.1}$$

where,

S_{out} is the output signal power measured in dBm.

S_{in} is the input signal power measured in dBm.
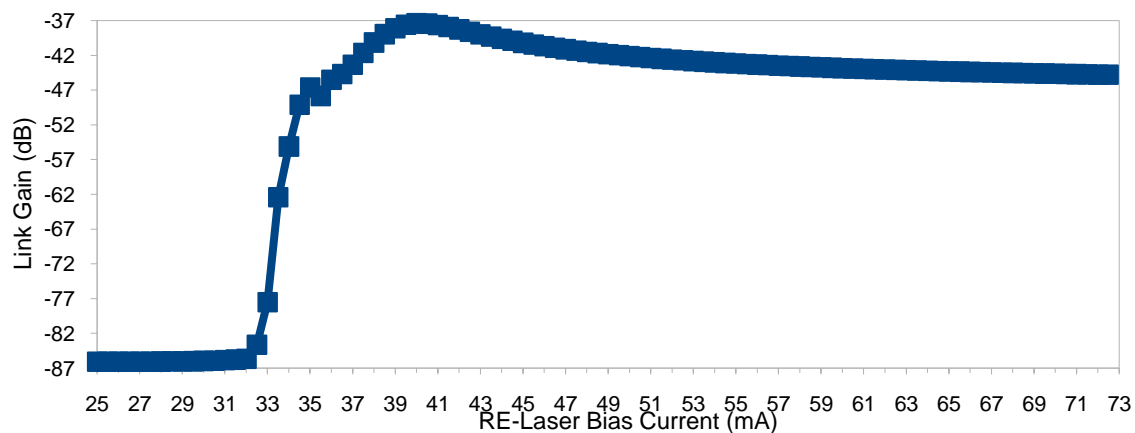
Figure 2.8: A graph showing link gain for a range of input bias current values

The input bias current parameter of the RE-Laser is the fixed level about which the sinusoidal waveform oscillates, it was varied from 25 to 72.5mA and the current amplitude was kept constant and the link gain was calculated. From the graph, it can be observed that the laser produces zero light power for the region before threshold current and shows a growing output up to 40mA before becoming nearly constant.

The same layout was used for the calculations of the current amplitude versus link gain calculations. The current amplitude is the maximum peak level that a sinusoid reaches from the bias during oscillation. Figure 2.9 shows the graph for the calculations.
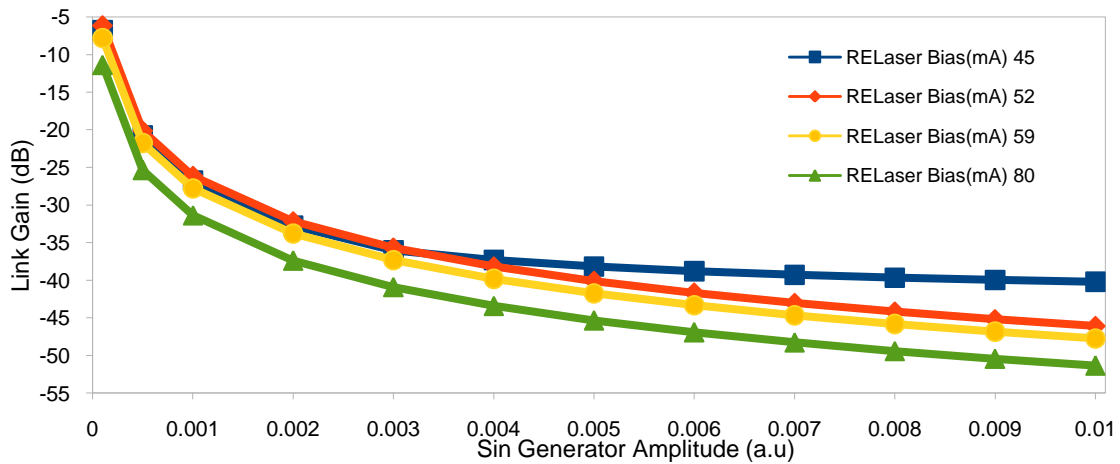
Figure 2.9: A graph showing the link gain for a range of input current amplitudes with the different bias values

The same parameters were used as in the previous calculations, however the bias current values were selected from the linear region in the LI curve that is 45, 52, 59 and 80mA. It can be seen from the plot that link gain decreases with the current amplitude.

The effect of different frequencies on the link gain is defined next, the same layout was observed and calculations were carried out. The frequency of the sin generator component was varied from 0.25GHz to 6GHz while the input bias current and amplitudes were kept fixed at 45mA and 0.01V respectively. The corresponding readings were carried out for optical fiber lengths of 10m, 10km, 50km and 100km.
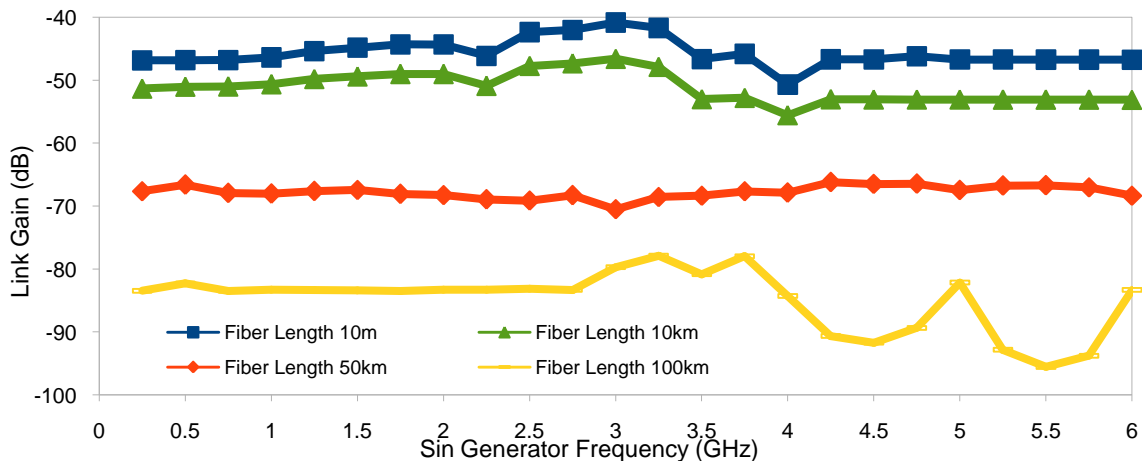
Figure 2.10: A graph showing the link gain for the range of carrier frequencies with the different fiber lengths

It can be observed from the graph in Figure 2.10 that the fiber has a fairly steady response for low frequency signals and for the shorter lengths of fiber. The 100km fiber exhibits large fluctuations at higher frequencies, although the difference in attenuation among the 50 and 100km fibers is 10dBm, it gets distorted at higher frequencies.

2.4.2 Vertical Cavity Surface Emitting Lasers (VCSELs)

The VCSEL component's modulation dynamics are modeled by the coupled rate equations that define the association among carrier, photon densities, optical phase and temperature. It includes thermal effects and parameter fitting based on the measured LI and IV curves.

For a modulated signal to be carried without distortion in order to preserve signal integrity, the L-I curve provides essential linearity characteristic of a VCSEL's output power for different levels of input current. The following layout is used for the verification of the VCSEL component's LI curve.
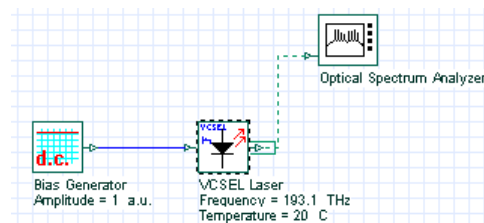
Figure 2.11: A layout for LI curve calculations of VCSEL

The global parameters are kept at default while the component values are also kept at default as shown in the layout above, the LI curve for the component is shown in the plot below which is nearly in accordance with the optisystem's LI curve graph available in the component properties.
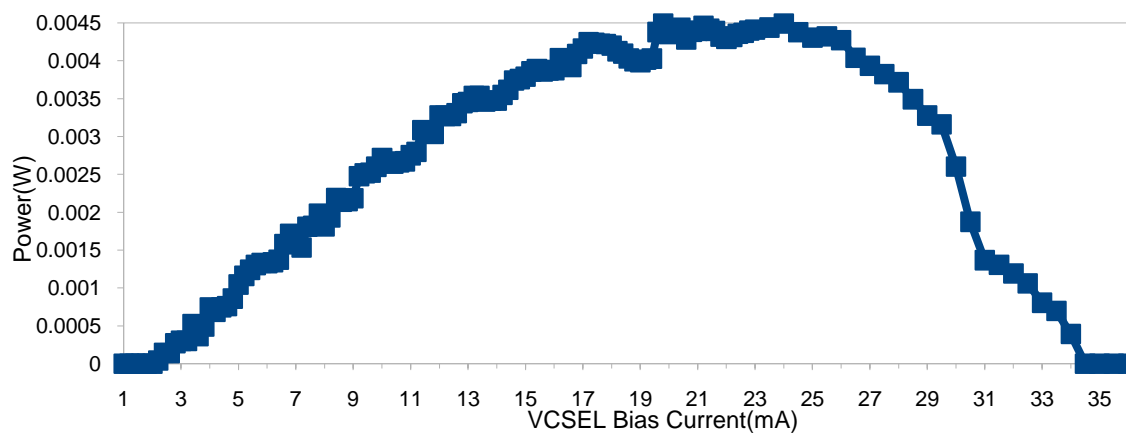
Figure 2.12: A graph showing the LI curve readings for VCSEL

As can be seen from Figure 2.12 that the VCSEL exhibits a threshold region up to 2.4mA bias current and the power output increases to reach a peak of 4.5mW at 20.2mA bias current and then decreases onwards down to minimum at about 34mA bias current before going back to zero output.

The input bias current readings against the link gain is plotted using the same layout as the RE-laser, except for the RE-laser is replaced with VCSEL as shown in the following layout.
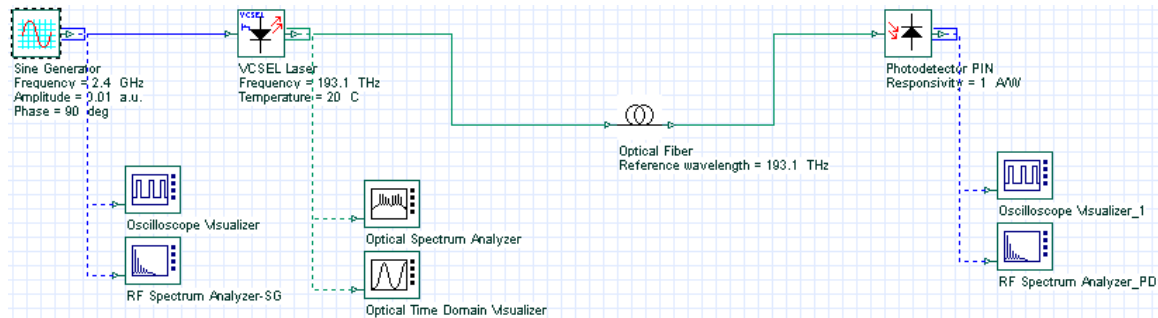
Figure 2.13: Layout for the calculations of VCSEL operating characteristics

The parameters for the components are as described in the layout while the global parameters are configured by setting a bit rate of 1.25 Gbps and a sequence length of 16 bits with 32 samples per bit providing a total of 512 samples. The length of the fiber is kept at 10 meters and the bias current values are changed from 1 mA to 34.5 mA. The graph for the readings is shown below.
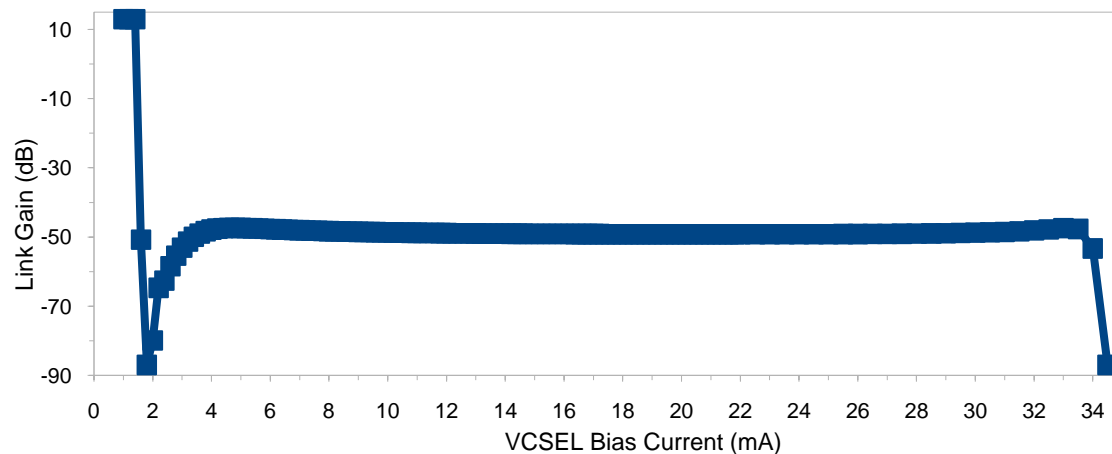
Figure 2.14: A graph showing the link gain for the range of VCSEL input bias currents

The VCSEL demonstrates zero output power for bias current values below threshold. For values above threshold, the link gain remains around the -50 dB value before dropping significantly at the same values as the LI curve. The small change of 1-2 dB in the link gain indicates that the sensitivity is not very much affected by this characteristic of the component.

Utilizing the same layout for simulations, the subsequent calculation of the link gain was carried out by varying the current amplitude, and the graph is shown in Figure 2.15.

For the simulations, the input bias current was kept at 5.4, 9.6, 13 and 19.6mA considering the linear regions obtained from the LI curve.
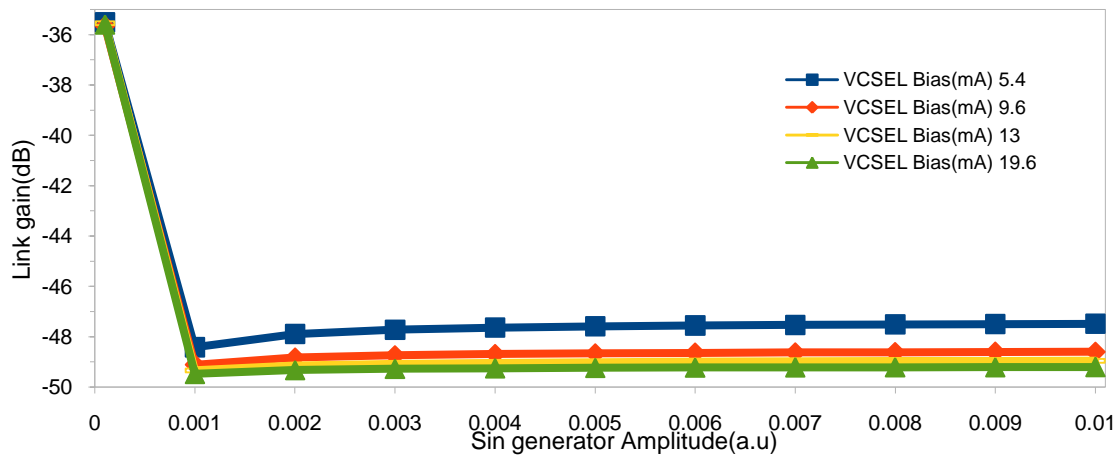
Figure 2.15: A graph showing the link gain for the range of input current amplitudes with different bias values for VCSEL

The graph shown above explains that the link gain remains reasonably constant with the changes in the current amplitude. The final characterization of the effect of sin generator frequency variations on the link gain is depicted in the graph shown in Figure 2.16. The calculations were done from the readings recorded from the same layout as of above and with the same configurations except for varying the sin generator frequencies and keeping the VCSEL bias fixed at 19.8mA.
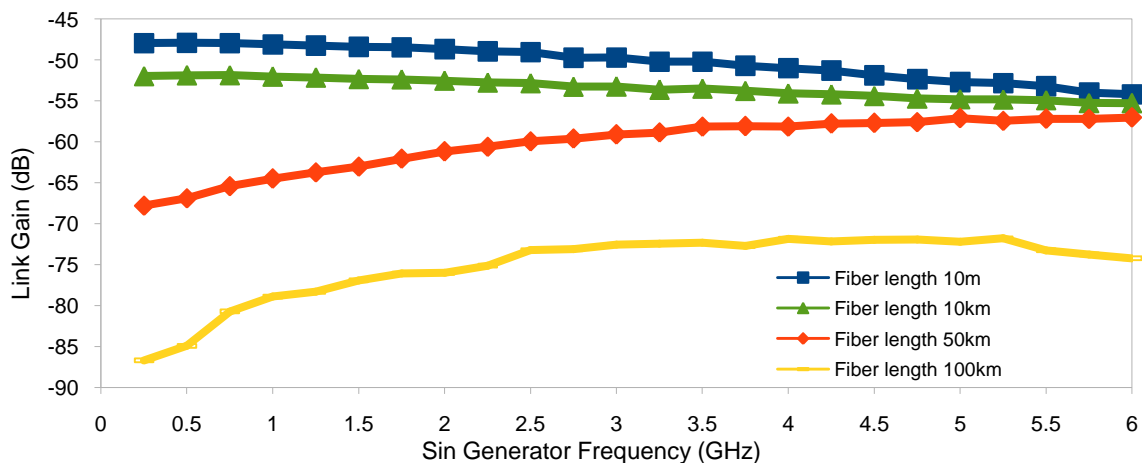
Figure 2.16: A graph showing the link gain for the range of carrier frequencies with different fiber lengths using VCSEL

The readings were carried out for fiber lengths of 10m, 10km, 50km and 100km with longer lengths i.e. 50 and 100km of fiber demonstrating the power changes of around 10 dB for the range of frequencies while the shorter lengths provide quite a steady output.

A p-doped, intrinsic, n-doped (PIN) type photodiode (PD) is used for the recovery of the modulated signal from the optical to the electrical domain. The PD's output current is proportional to the optical

power of the incident light wave and, as a result, is also proportional to the RF signal [18]. The generated RF signal would carry the same data (preserving the modulation) as that of the modulating RF signal carried at the time of optical carrier modulation at the source. It is a simple yet efficient method and is denoted as direct detection (DD).

The major advantage of direct intensity modulation is its simple implementation. If the consideration of a linear optical to electrical converter is made and the dispersive effect of the fiber is neglected, the system becomes transparent to the RF signal, performing attenuation or amplification [8].

External modulators are considered to have a wider bandwidth and a lower noise figure and only external modulation of a high-speed MZM permits modulations of RF signals with frequencies up to 100GHz [19]. Yet, they usually need high drive voltages, which lead to very costly drive amplifiers. Moreover, analog applications are more sensitive to the nonlinearities therefore the strict linearity requirements of the system components has to be catered in the IM/DD scheme [18].

2.5   Benefits and Applications of the RoF Technology

The RoF technology is a well known platform for the distribution of wireless signals representing different standards. Some of the important contributions of RoF technology are listed in Table 2.1.

Table 2.1: Benefits and Applications of RoF technology

Benefits	Applications
• Radio coverage improvements.	The bandwidth generous fiber optic provides the high bandwidth wireless systems the required platform to expand.
• Transparency of the system to modulations carried by radio waves.	One of the most important applications for the RoF technology is considered to be the distributed antenna systems (DAS) where multiple standards can share a single platform for communication and a center for data processing could cater to multiple remote antenna units [6, 20, 21].
• Simplified remote antenna units (RAU).	Simplification of the RAU allows for easier and flexible installations and less equipment and maintenance costs [10, 22].
• Dynamic resource provision and long-term optical infrastructure.	The RoF systems can provide a long-term infrastructure for communication because of its capability of joint processing of signals and it can be equally productive for the next generation standards [6].

2.5.1 Distributed Antenna Systems (DAS)

A growing market for the RoF technology is the distributed antenna systems (DAS) which employs optical transmission links effectively carrying radio signals to connect a central unit (CU) incorporating radio base stations (BS); to some remote antenna units (RAU) as shown in the example in Figure 2.17.
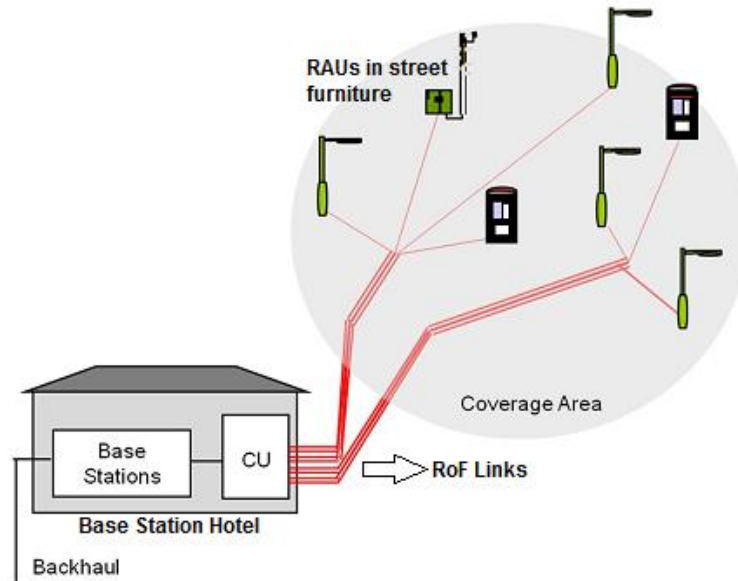
Figure 2.17. A city center design of the DAS using RoF links [20]

Therefore, the short range communication areas like malls, offices and transport centers are provided with immaculate coverage and a defined capacity [23]. Figure 2.17 is a depiction of a city center design based on DAS topology where the BS and the CU are housed in a structure referred to as a base station hotel, and the RoF links connect the CU to the street objects containing the RAUs [20].

2.6 Limitations of the RoF Technology

Analogue modulation and light detection in principle, make RoF an analogue transmission system. Therefore, factors affecting a signal in analogue communication systems such as noise and distortion, are important in RoF systems as well. The O-E and E-O conversion noise, the amplifier's thermal noise, and the fiber's dispersion are some of the basic factors contributing to the signal impairment. RoF systems using SMFs might have limited fiber link lengths due to chromatic dispersion and may also suffer from phase de-correlation leading to increased RF carrier phase noise. In a MMF based RoF systems, modal dispersion severely limits the available link bandwidth and distance [10].

Next generation systems for the wireless transmission would require more noise and distortion control for the RoF links used in the DAS [20].

3   Orthogonal Frequency Division Multiplexing Techniques

3.1   Introduction

The OFDM technique is based on the frequency division multiplexing (FDM) concept in which a serial data stream is divided into multiple parallel streams and then each of them is modulated on multiple lower frequency carriers placed adjacent to each other spanning within the bandwidth of the transmission medium. With many subcarriers, data-rates similar to single-carrier modulation can be achieved. In OFDM the sub-carriers; also known as tones, are orthogonal to each other, they use digital data modulation formats such as phase-shift keying (PSK) or quadrature amplitude modulation (QAM) schemes.

The OFDM concept is based on the use of multiple frequencies for transmission, the same concept which was already under military usage during the 1960's [24, 25]. In 1966, the concept of orthogonal frequencies was proposed and then patented by Chang *et al.* [26]. The complexity in implementing an OFDM modem made it less utilized. The different forms of the fourier transform (FFT, DFT) were proposed for generating orthogonal signals around the 1970's which hugely simplified the OFDM modems [27, 28]. In 1980, Hirosaki *et al.* [29] suggested an equalization algorithm to contain both inter symbol and inter subcarrier interference caused by the channel impulse response or by time and frequency errors, while another important part of OFDM; the cyclic prefix was also proposed in the same year [30].

In the year 1985, Cimini *et al.* [31] published the first analytical results on the performance of OFDM modems in mobile communications. Practical usage of OFDM began in the same period with another valuable factor of forward error correction (FEC) being joined to the OFDM [32]. the relationship between the coded data and the OFDM brought the term coded OFDM to existence [33].

OFDM is now the building block of many telecom standards like wireless LANs (WLAN) [34]. Also, it is widely used for television (digital video broadcasting - DVB) and radio [35]. OFDM with its applications is still considered a modern scheme with an ever increasing research base and evaluation being carried out with different mediums like optical wireless, optical fiber (SMF/MMF) and plastic optical fibers. The components and key factors contributing to OFDM systems like orthogonality, fourier transform and cyclic prefix [33], are discussed next.

3.2   Orthogonality - from FDM to OFDM

A number of signals or subcarriers combined in a set are mathematically known to be orthogonal, if the inner products between all of them equal zero. The orthogonality is a property that provides no crosstalk (a signal's channel distorting other channels) between the sub-channels therefore, demodulation of the subcarriers is possible without inter-carrier interference (ICI) [8].

Subcarrier orthogonality is observable in the time domain as every single subcarrier is required to have an integer number of cycles during each OFDM symbol interval, or, the difference in number of cycles should be at least one between adjacent subcarriers.

For the frequency domain, orthogonality between subcarriers is observed by the maximum amplitude of a subcarrier occurring at its own center frequency and a corresponding null for all the remaining subcarriers as shown in Figure 3.1.
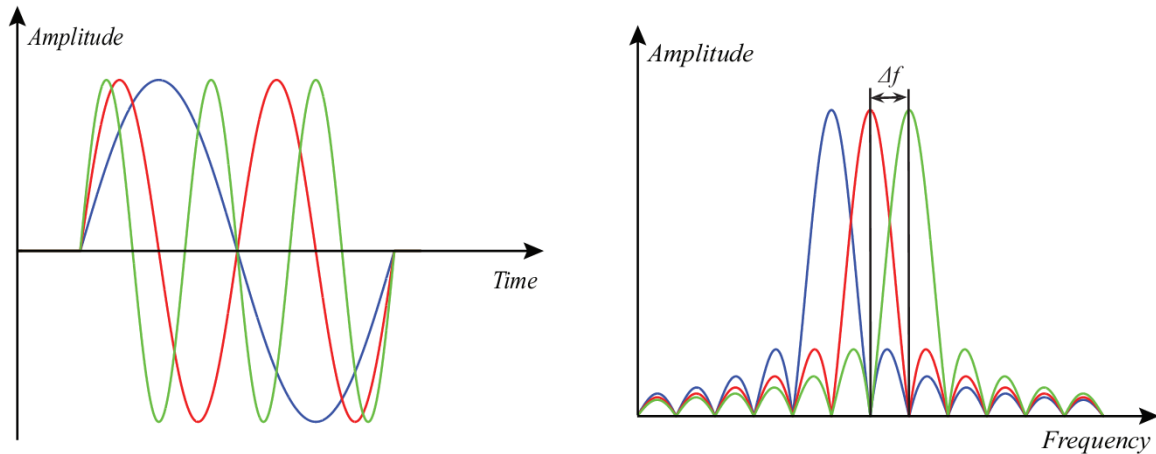
Figure 3.1: Time domain and Frequency domain representation of three subcarriers that constitute a baseband OFDM symbol for subcarrier frequency spacing of Δf [8]

This also defines the calculations done by the OFDM receiver which calculates the spectrum values of the individual subcarriers at the maximum points and therefore it is able to recover each subcarrier without the ICI interference from the remaining subcarriers. Many different techniques like time-division multiplexing (TDM) and typical FDM used by the communication systems are naturally orthogonal. A time slot is specified for every subchannel in TDM, while a simple FDM system places the subchannels in adjacent spaces in frequency with guard bands as shown in Figure 3.2. Therefore, two signals can have orthogonality if they do not overlap either in time or in frequency domain [8].
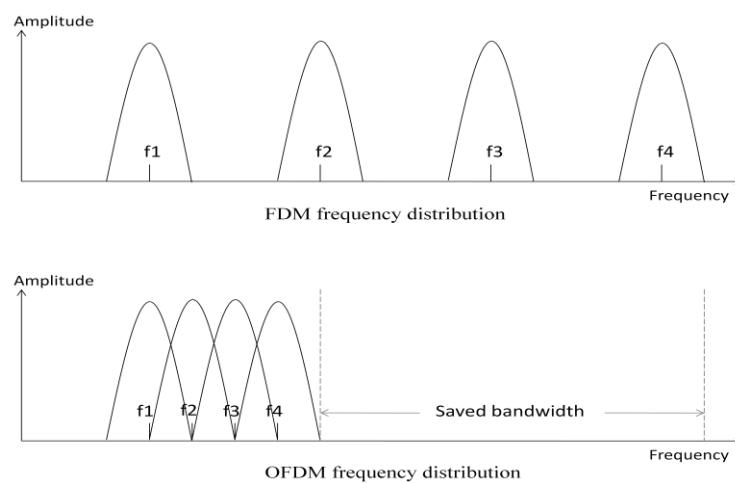
Figure 3.2: Bandwidth efficiency in OFDM compared to FDM

Orthogonal placement of sub-carriers is performed by OFDM resulting in a significant saving of the bandwidth as shown in Figure 3.2, where individual carriers in the FDM along with their respective guard bands have large separations, however, all of the same carriers were placed together in an orthogonal manner in the OFDM, creating more space in the spectrum.

Carrying the FDM example further, the principle task of any FDM system is to distribute the information into N parallel streams, each stream then modulates a carrier using a modulation technique. The frequencies of adjacent carriers are spaced at Δf, so the total signal bandwidth is $N\Delta f$. The transmission of all N modulated and multiplexed signals is done over the channel, and N branches of receiver are used for extraction of information. Then, to rejoin the N parallel information streams, a multiplexer puts them together into a high-rate serial stream [36]. This brings us to the OFDM system description which roughly has the same architecture as of a FDM system.

3.3   OFDM System Description

The composition of an OFDM system includes the transmitter and receiver sections, which consist of different modules as shown in Figure 3.3. The serial data after processing (for e.g. interleaving, coding) is mapped by a modulator (for e.g. QAM) and the symbols created are then branched out into N parallel sections and grouped by a serial-to-parallel converter (S/P) before being sent to the IFFT for the generation of time-domain samples for the signal and then for the addition of guard interval or cyclic prefix. The samples are then arranged in a serial sequence by a parallel-to-serial converter (P/S) and then sent to the digital-to-analog converter (DAC) and an optional up-converter before being transmitted on the channel.
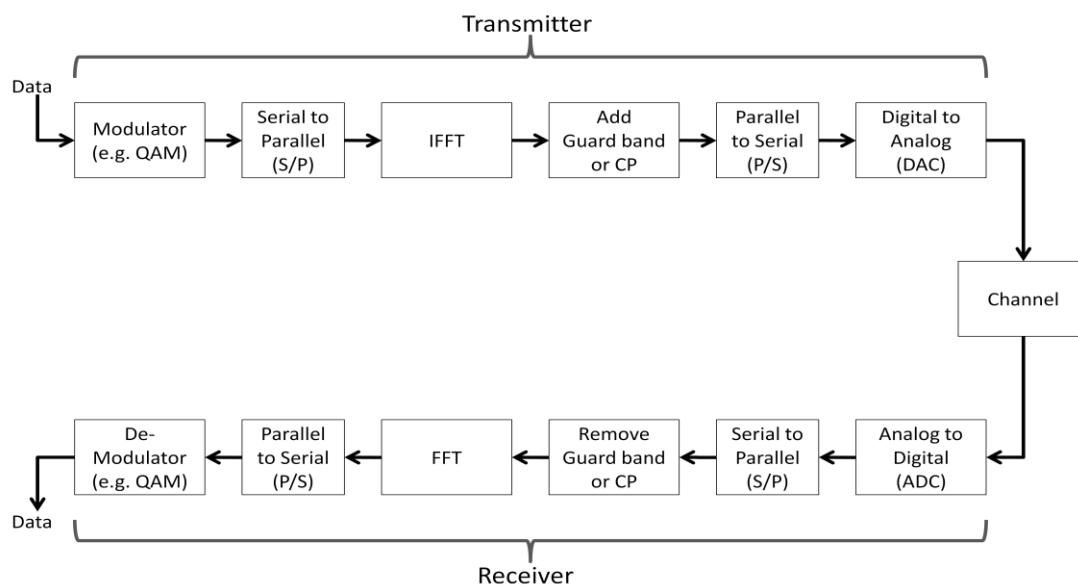
Figure 3.3: A block representation of an OFDM system[33]

The receiver section consists of about the same modules but the process is performed in reverse with the bandpass OFDM signal being down-converted and then sent to analog to digital converter (ADC) and the corresponding samples are then distributed in parallel by the S/P converter and the removal of guard interval or cyclic prefix is done before the FFT block recovers the sequence from N length of samples. This sequence is sent to the P/S converter and later demodulated by the demodulator to gather the data efficiently that was sent from the transmitter.

3.3.1 Modulation Techniques

In an OFDM system, the importance of the choice of modulation technique becomes evident as the prerequisites involving power efficiency and spectrum utilization can be influenced directly by the modulation chosen. The mapping of data words to a specific real (in-phase) and imaginary (quadrature) point in the constellation is referred to as modulation. For e.g. 16-QAM uses 4-bits for one symbol which is mapped to one unique location on constellation. The type of modulation can be specified by the complex number [37],

$$d_n = a_n + jb_n \tag{3.1}$$

where

a_n and b_n are symbols that can take on values of ± 1, ± 3, ... etc. depending on the number of signal points in the signal constellations [29].

For example, a_n and b_n can be selected to (± 1, ± 3) for 16-QAM and ± 1 for QPSK, as shown in the constellations available from Matlab in Figure 3.4.
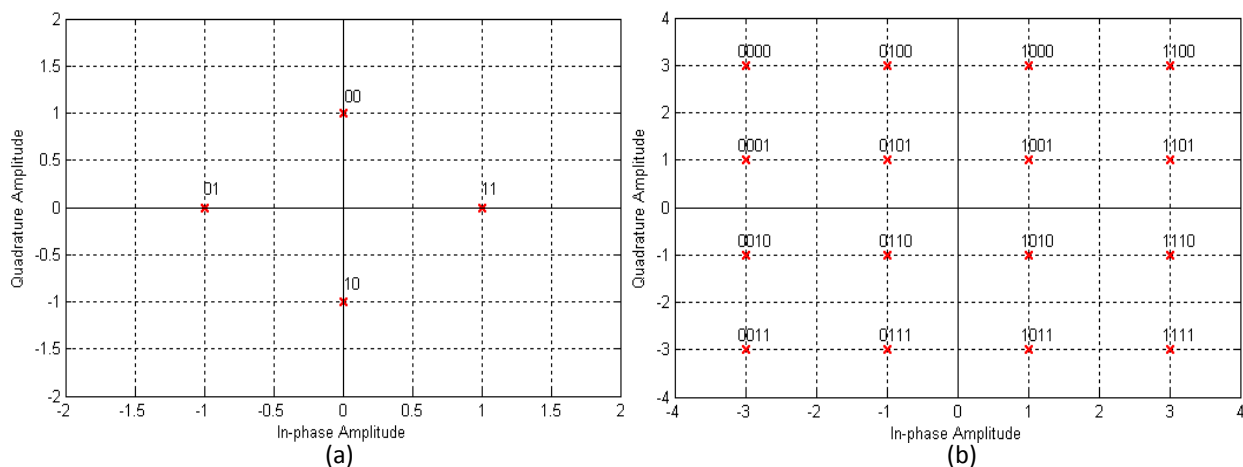
Figure 3.4: Constellation diagrams for (a) QPSK (b) 16-QAM

General choice for modulation of subcarriers is QAM or PSK [36]. For practical implementations, 4 to 64 level constellation sizes are typically used in QAM systems [29, 33]. The PSK scheme is compatible with

OFDM, but is seldom used as it does not have a constant signal envelope and, for large constellations, has smaller distance between constellation points, having sensitivity to noise, contrary to PSK in systems using one carrier [33].

Summarizing the concept, it is observed that the modulation schemes being utilized on the subcarriers differ by the tradeoff between the fast data-rate and powerful transmission [37]. The complex numbers sequence output from the modulators or constellation mapping is then changed over in a S/P converter to provide the required vector for input to the IFFT.

3.3.2   Discrete Fourier Transform

The concepts of performing fourier transforms for the modulation and demodulation were first introduced by Salz *et al.*[27] and then by Weinsten *et al.* [28] in the time around 1970's. The discrete fourier transform for the operation of modulation and multiplexing functions together is the most important part at the transmitter side of an OFDM system. The sequence of symbols is divided into different slots in the frequency domain and an IFFT is used to modulate the data into the time domain. At the receiver side, the samples received are fed to an FFT block for the demodulation and demultiplexing and for the original data to be reconstructed, with the output being real valued if used in conjunction with imposition of conjugate symmetry at the transmit section. It is not unjust to ascertain that OFDM systems are set apart from the single carrier systems by the implementation of the fourier functions at the transmission and reception [33].

For an OFDM system, ideally dividing the data into parallel requires many subcarriers having narrow bandwidths so that each subcarrier might experience a flat fading, this requirement might add up to the complexity of signal processing at both sending and receiving ends. For a better understanding, we consider the sequence of symbols to be transmitted; being input as $\{X_n\}_{n=0}^{N-1}$ to the IFFT at the transmitter side operations, and the data after modulation is expressed in time domain as [38],

$$x(t) = \sum_{n=0}^{N-1} X_n e^{j2\pi f_n t} \tag{3.2}$$

where,

X_n = sequence of symbols being input

N = number of subcarriers

f_n = frequency for the nth subcarrier

Also,

$$f_n = f_o + n\Delta f \tag{3.3}$$

where,

Δf = frequency spacing between subcarriers

If we sample $x(t)$ at an interval of $T_{sa} = T_s / N$, then we can write Eq. 3.2 as,

$$x_k = x(kT_{sa}) = \sum_{n=0}^{N-1} X_n e^{j 2\pi f_n \frac{kT_s}{N}} \tag{3.4}$$

In the absence of loss of generality, defining $f_o = 0$, we get the above equation simplified as,

$$x_k = \sum_{n=0}^{N-1} X_n e^{j 2\pi \frac{k n \, \Delta f \, T_s}{N}} \tag{3.5}$$

and for the condition of orthogonality, $\Delta f \, T_s = 1$, so the Eq. 3.5 becomes [38],

$$x_k = \sum_{n=0}^{N-1} X_n e^{j 2\pi \frac{kn}{N}} \tag{3.6}$$

$$x_k = IDFT \{X_n\}$$

The equivalence to the inverse discrete fourier transform (IDFT) here implies the use of the DFT at the receiver, and because the forward and inverse transform roughly employ the same circuits, a transceiver can be constructed with simple changes for performing both modulation and demodulation. The representation of the forward and inverse DFT varies hardly without any major changes among the different literature so in the same way as its inverse was defined, the forward FFT is defined by [38],

$$X_n = \frac{1}{N} \sum_{k=0}^{N-1} x_k e^{-j 2\pi \frac{kn}{N}} \tag{3.7}$$

As discussed previously, the requirement of many subcarriers was ideal for OFDM but required complex signal processing, however, with the fourier transform implementation this process is fairly simplified and the mathematical calculations involving multiplications are diminished from N^2 to $N/2 \log 2N$ where N is the number of steps. Therefore, an improved processing time is obtained [38].

3.3.3   Guard interval

The transmission of the OFDM signals through dispersive channels or through channels having multiple routes or paths is the reason for the occurrence of inter carrier interference (ICI) and Inter symbol interference (ISI) respectively. Multiple transmitted signals after getting reflected and scattered from the

surroundings, reach at the receiver with delays and impact the synchronization and cause the frequencies to distract from their orthogonal nature, while the spreading of symbols causes interference amongst consecutive symbols in a dispersive channel.

An important preventive measure is to insert guard intervals between the OFDM symbols so as to protect the symbols from over lapping each other, this 'silent' guard interval can be added at the start of every OFDM symbol and thus ISI can be remedied as far as the channel dispersion remains shorter than the guard interval, but unfortunately ICI cannot be overcome [8]. The conception of cyclic prefix which is considered a type of guard band provided the solution to ICI, we discuss it next.

3.3.4   Cyclic Prefix (CP)

In the year 1980, Peled *et al.* [30] revealed the remedy to the ICI by conceiving the cyclic prefix option as the guard interval. The cyclic prefix is a unique method for the protection of the orthogonal property among the subcarriers and for prohibition of ISI in the middle of sequential OFDM symbols. The cyclic prefix is an extension of the OFDM symbol which is copied from the end and appended as guard interval to the beginning of the symbol as illustrated in Figure 3.5.
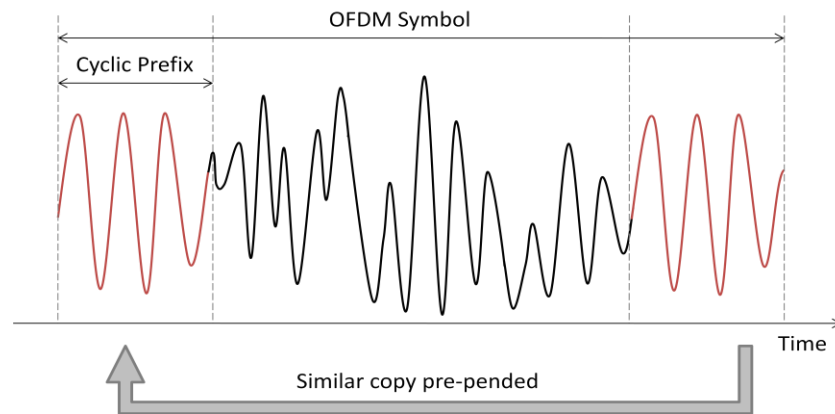
Figure 3.5: Addition of the cyclic prefix in an OFDM symbol

Each OFDM symbol is cyclically extended and added as a prefix to itself but even with redundancy, the efficiency of the transmitting OFDM symbols is reduced by a factor of, $N/N + N_g$ in a N sample OFDM sequence having N_g samples of guard interval. To diminish this deficiency, deploying a larger number of subcarriers can be beneficial [36].

CP can efficiently diminish the ISI and ICI to the negligible levels with proper alignment of the receiver FFT window with the received signal's main symbol period and by defining a CP which should not deceed the delay spread [8, 33]. After inserting the CP, the OFDM sequence is changed over to serial

arrangement of the symbols by the parallel to serial converter, later to be converted to analog format and for up conversion if required.

3.3.5 Digital-to-Analog and Analog-to-Digital Converters

The OFDM symbols generated by the modulator are the baseband signals in the digital form and for these signals to traverse the channel, necessary conversion to analog and up conversion have to be performed before it is placed on the channel for transmission.

In an OFDM system, the digital to analog converter (DAC) and analog to digital converter (ADC) are the components that carry out the conversions of data from digital to analog domains and vice versa. A specific time variant filtering is usually applied to the OFDM symbols for minimizing the sidelobes, including an occasional up-sampling of the digital signal before being changed over to analog for a less complicated filtering which can be performed in either of the analog or digital domains [33].

The conversion from digital to analog and vice versa is also significant for the pace at which processed data can be transferred, therefore the use of the simple signal processing levels and components can add up to the overall performance of the system.

3.4 Advantages and Disadvantages of the OFDM

In comparison to systems employing modulation techniques involving one carrier, OFDM modulated signals usually perform better in time-dispersive channels. But, with the advantage of a multi-carrier transmission, the OFDM technique is drawn back by the disadvantage of a high peak-to-average power ratio (PAPR) and a high sensitivity to nonlinear distortion, susceptible to synchronization errors, specially frequency offset errors [8].

Some advantages along with a few drawbacks of the OFDM technique are briefly mentioned in the following table.

Table 3.1: Advantages and disadvantages of the OFDM.

Advantages	Disadvantages
• High efficiency in frequency spectrum utilization, the bandwidth is optimally used with multiple carriers providing high data rates in the limited bandwidth. • Orthogonality among the subcarriers allows for a stronger defense against narrow-band co-channel interference or inter channel interference (ICI).	• Sensitive to frequency synchronization problems and Doppler shift. • OFDM is sensitive to Carrier Frequency Offset (CFO) and phase noise. The local oscillator phase noise or frequency mismatch between the transmitter and the receiver, imply a loss of orthogonality between subcarriers and deteriorates the performances of the system.

• The modulation and multiplexing scheme of OFDM is carried out by implementing FFT, which provides simplified Digital Signal Processing (DSP) at the transmit and receive sections. • OFDM is also flexible in implementing independent modulation schemes on the subcarrier according to the channel situation with the option for different subchannels for layered services [29].	• OFDM systems are reactive to the variations between the I and Q channels, which can cause mutual interference between pairs of symmetric subcarriers. • High Peak-to-Average Power Ratio (PAPR) which occurs when subcarriers are added constructively causing large peaks in contrast to the average power and eventually imposing strong constraints on the modulation index of the optical source.

For its rugged yet somewhat complex structure, OFDM is still considered the viable choice for most of the high speed communication standards today and it will continue to be used to provide even more efficient mode of communication like the basis for a multiple access scheme like OFDMA [20].

3.5   Coded OFDM

Distribution of the information sequence between different frequencies, provides a useful option for communication of signals on a frequency selective channel but that might not restrain the fading on its own. Various subcarriers can be disturbed by fading occurring at separate frequencies and that requires for the implementation of coding procedures to further enhance the shielding of the data [37].

The process of coding the sequence is conventionally done before performing interleaving to contain the adjoining subcarriers from falling into the frequency slots which are fading. Every OFDM system employs some error correction and detection configuration, for e.g. digital audio broadcasting (DAB) and digital video broadcasting (DVB) benefit from two layers of interleaving and coding for getting better bit error rates (BER) over noisy channels [33].

The conception of combining error correction with OFDM systems was brought forward in 1987 by [32], later known as coded OFDM (COFDM). The COFDM design encodes the binary sequence and performs interleaving of the coded data, which is useful for rectifying of errors in channels with low gain.

A coding scheme called Concatenated coding incorporates a block and convolution coding procedure plus interleaving. Turbo codes are the new age of parallel concatenated codes which assure encouraging applications with OFDM in the future [39], a simulated example proposes optical OFDM along with turbo codes for a less erroneous communication [40].

3.6   Optical OFDM

The initiation of OFDM for the optical domain took place in the year 1996, and provided a consistent

research attraction since then. The optical OFDM is basically defined by two techniques, the direct detection optical OFDM (DD-OOFDM) and the coherent optical OFDM (CO-OFDM) [41]. In the common OFDM systems the electrical medium is able to carry both positive and negative values of the signal while the optical medium uses intensity modulation of light which can carry only positive values [33], that being the reason for division of optical OFDM according to detection techniques.

For this study direct detection (DD-OOFDM) scheme is implemented, the OFDM transmitter is responsible for the generation of electrical OFDM which is up converted into the optical domain by the electrical to optical (E/O) up converter and performs the modulation of light intensity which is propagated along the optical fiber. At the receiver, the optical signal is changed over to electrical by an optical to electrical (O/E) converter, usually a photodiode. Direct detection schemes are also the mainstream application of the optical OFDM in the past twenty years, while its counterpart coherent detection is also researched extensively [41].

4   Turbo Codes

4.1   Introduction

The channel is a mode of conveyance for sending coded messages from one end to another, and for radio channels the noise and interference impact the waveforms carrying the information, hence causing errors at the receiver and decoder sections. For any communication, the transmitted signal power, the channel bandwidth, and the power spectral density of noise are the characteristic values for determining the signal to noise ratios (SNR), which in turn can define the extent to which noise can influence a signal. For specified signal to noise ratios, the integrity of information can be improved by implementation of forward error correction (FEC) [42].

The FEC channel coding guards the information against channel perturbations by the addition of organized redundancy to the original sequence that is to be transmitted. The addition of parity at the transmitter and the benefit from redundancy in decoding allow for error corrections and provide reliability to the channel [43]. Basic categories of channel codes are block codes and convolutional codes.

The block and convolutional codes are distinct in the encoding concept. The block codes perform coding of information in blocks of a particular size, parity bits are added after information bits. Convolutional codes continuously perform coding on the sequence of incoming information bits according to some rule, instead of doing it block by block.

The transmission of a stream of message and decoding the received randomly corrupted messages with utmost efficiency was the theory for an optimum code put forward by Shannon [44]. Taking a look at the redundancy added by the channel encoders, it is observed that information can be detected and also corrected with random error patterns. Error correcting codes, the channel codes that perform correction of the inaccurate bits, also accommodate the turbo codes[45].

4.2   The advent of Turbo Codes

The definition of a new era of channel coding took place in the year 1993, when the turbo codes were introduced by Berrou *et al.* [46] in their unprecedented paper, whose conclusions were first doubted by the researchers and designers but today they are accepted largely. The paper provided the results for a possible communication around about the lower limit of an additive white gaussian noise channel, predicted by Shannon.

The selection of encoders and decoders for coding and efficient decoding was also contributed with the description of basic principle of turbo codes. Turbo coding is carried out by two encoders which encode the same message in two different forms, the decoders are also setup in a way where every decoder performs its share of decoding on the concatenated codeword. The sharing of information regarding the decoding results is carried out between the decoders to correctly identify the codeword, which also

defines the 'turbo' concept in the sense that iterative decoding in turbo codes allows for the output from one unit to be input to the next one over and over like a turbo combustion engine as shown in Figure 4.1. Therefore the turbo decoding and iterative decoding are considered to be same methods that define the basic concept of turbo codes.
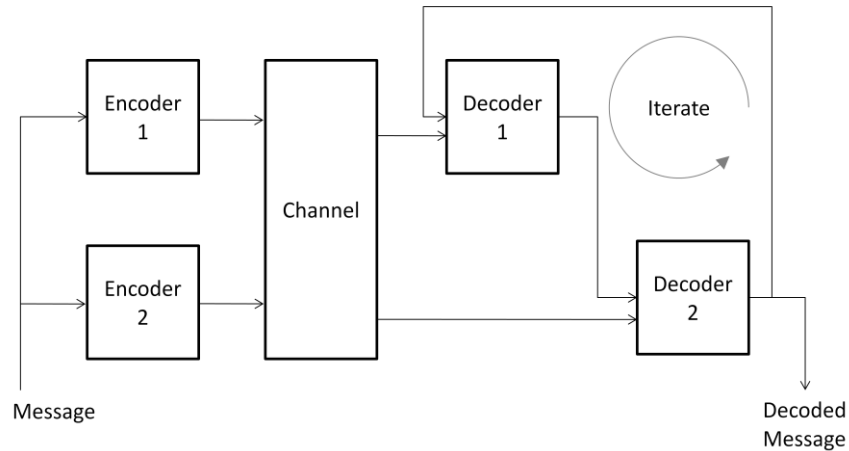
Figure 4.1: A basic turbo coding and decoding concept

With the description of turbo codes, another important contribution was with the construction of encoders where parallel concatenation of recursive convolutional encoders was done. This combination of encoding and decoding allowed for assembling large and composed codes combined with efficient decoding. Further research is still being done with various structures and combinations of encoders being placed, for e.g. serial concatenation, hybrid concatenation and others with differing characteristics and behaviors. This research is carried out with respect to the original encoders presented in the publication [46] stated before, with two parallel concatenated convolutional encoders. As discussed before the basic schemes for channel coding include block codes, but the next section focuses on convolutional codes because turbo codes were first implemented with the same.

4.3   Turbo Encoder Assembly

Turbo codes were presented with the combination of two integral encoders concatenated in parallel and were accompanied by an interleaver and a puncturing and multiplexing unit, therefore the three blocks compose the basic structure of a turbo encoder section. The interleaver is used to rearrange the sequence for the second component encoder as shown in Figure 4.2.
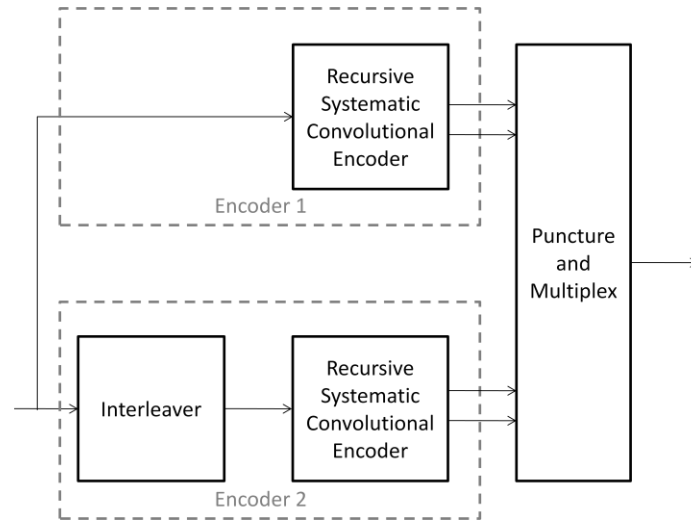
Figure 4.2: A block diagram of Turbo Encoder

The receiver block in turbo codes consists of the same amount of decoders as on the encoder side, with each of them working on the same information. This type of structure is called parallel concatenated convolutional code (PCCC).

4.3.1   Convolutional Encoders

The coders composing the turbo encoder block are recursive systematic convolutional (RSC) encoders. The recursive part is the feedback and the rest is a systematic convolutional encoder, which use information sequence as a part of the codeword by employing a direct connection from input to the output. As can be seen in Figure 4.3 that two bits of codeword are created for every input bit, these two bits are called systematic and parity bit.
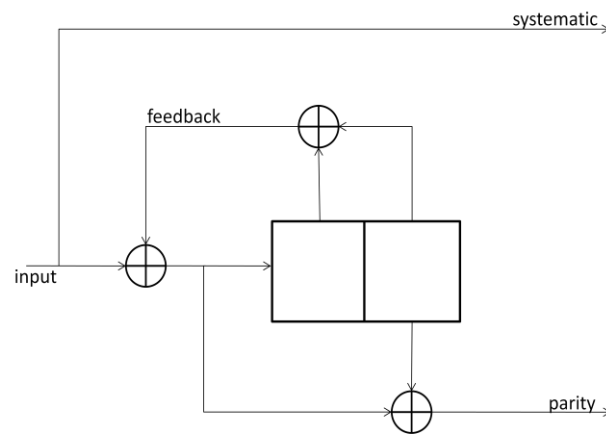
Figure 4.3: A recursive systematic convolutional (RSC) encoder with $(111)_2$ as feedback, and $(101)_2$ as parity polynomial

For both the convolutional and block codes discussed above, a parameter called the code rate is defined as the ratio of input information bits *(k)* to the coded bits being output (*n*), that is, R = k/n[45].

A convolutional encoder encodes *k* information bits to *n* code bits in each time step, with *n* > *k*. The encoder in Figure 4.3 has *k* = 1 and *n* = 2, so the code rate is R = 1/2.

Industrial representation of the encoders is usually done by (*n,k,m*) or (*n,k,L*) where *n* and *k* are the output and inputs respectively whereas *m* and *L* are respectively the number of memory registers and the constraint length. The constraint length parameter is defined in various forms in the literature available, but the definition that can be deducted from the originally proposed turbo codes is that it is the maximum number of symbols in a single output stream that can be affected by any input symbol [47], it gets represented by *K*, while *M* is the memory.

$$M = K\text{-}1 [46] \tag{4.1}$$

$$K = M+1 [47] \tag{4.2}$$

where,
K = constraint length, and *M* = memory

Also with the help of this parameter, the encoders can be represented as a state machine with L-1 states [48], here the constraint length being represented by *L*. Another significance of the RSC codes is that they are not memory-less, the past values of information are responsible for the coded bits being output at every time step. They differ from block codes, as the block codes are memory-less. The fact that the convolutional codes have memory provides efficient operation, when *k* and *n* are pretty small whereas, the block codes require long block lengths (e.g., reed-solomon code used in CD drives has *N* = 2048), because they are memory-less and their performance improves with block length.

4.3.2   State and Tree Diagrams

Compact representations of the functions or characteristics of convolutional codes can be done by the matrix, state and trellis diagrams. Each of them is discussed briefly below.

Using a polynomial *D* with octal representation to describe the encoder is one of the basic options where operator *D* shows a delay of one symbol time while D^n shows a delay of n symbol times. In Figure 4.3, the parity bit is explained as a function of memory registers by the polynomial $1+D^2$, likewise the feedback can be defined by the $1+D+D^2$ polynomial. The encoder's generator matrix or transfer function matrix [47] can be scribed in polynomial form as G(D) = (1 ($1+D^2$ / $1+D+D^2$)). The binary and octal representation of the coefficients can be done for both parity and feedback polynomials, with binary rendition of 101_2 and 111_2 while in octal, 5_8 and 7_8 defining the parity and feedback respectively for the encoder in Figure 4.3. Various polynomials can be selected for a specific order of code which differ in their error shielding properties. With complex computations some good polynomials have been listed for various rates [49].

State diagrams are a suitable method for defining convolutional encoders where each state relates to the contents of memory registers (*M*) and transitions from one state to another are labeled with input and parity bit matching to the state shift. With every incoming bit, the changing states of encoder define the initial condition on which the output is dependent.

Thus, a time-invariant q-ary encoder can be accepted as a finite state machine (FSM) with q^M states [47]. The diagram is constructed by circles and lines, the circles are the states and the lines show the state transitions with the input and output labeled above them as shown in Figure 4.4.
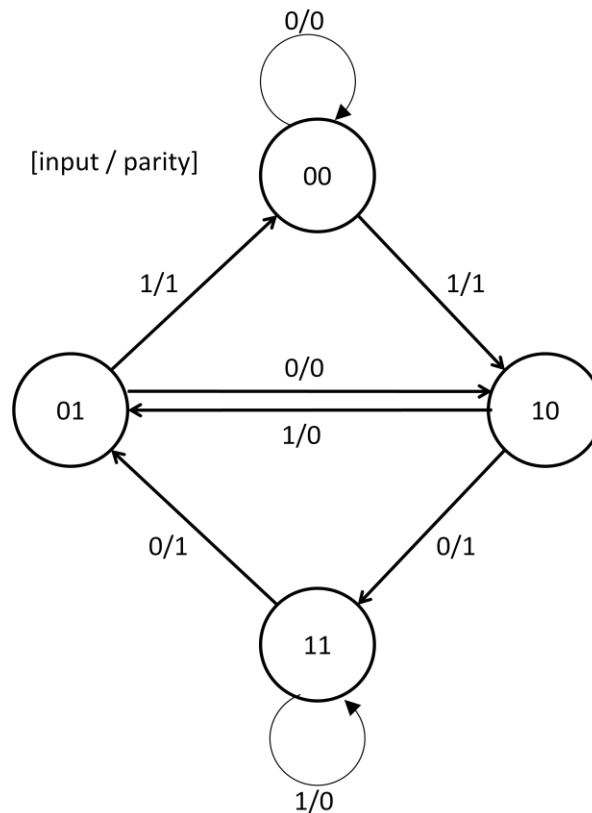
Figure 4.4: State diagram for the convolutional encoder in Fig. 4.3 [45]

State diagrams depict the encoder behavior for the complete time period, but a convenient option for decoding convolutional codes is to exhibit all of the encoder states for every time frame, this diagram is known as a trellis diagram. The trellis might appear difficult to understand but it is a rather descriptive embodiment of the previous states of encoder. Also, it always starts from the state zero at zero time as the root node [47].

The construction involves lining up all the possible q^M states vertically and then connecting them to other states accordingly with respect to the input bit at specific time frames placed horizontally, and labeling each path with output or both input and output as shown in Figure 4.5.
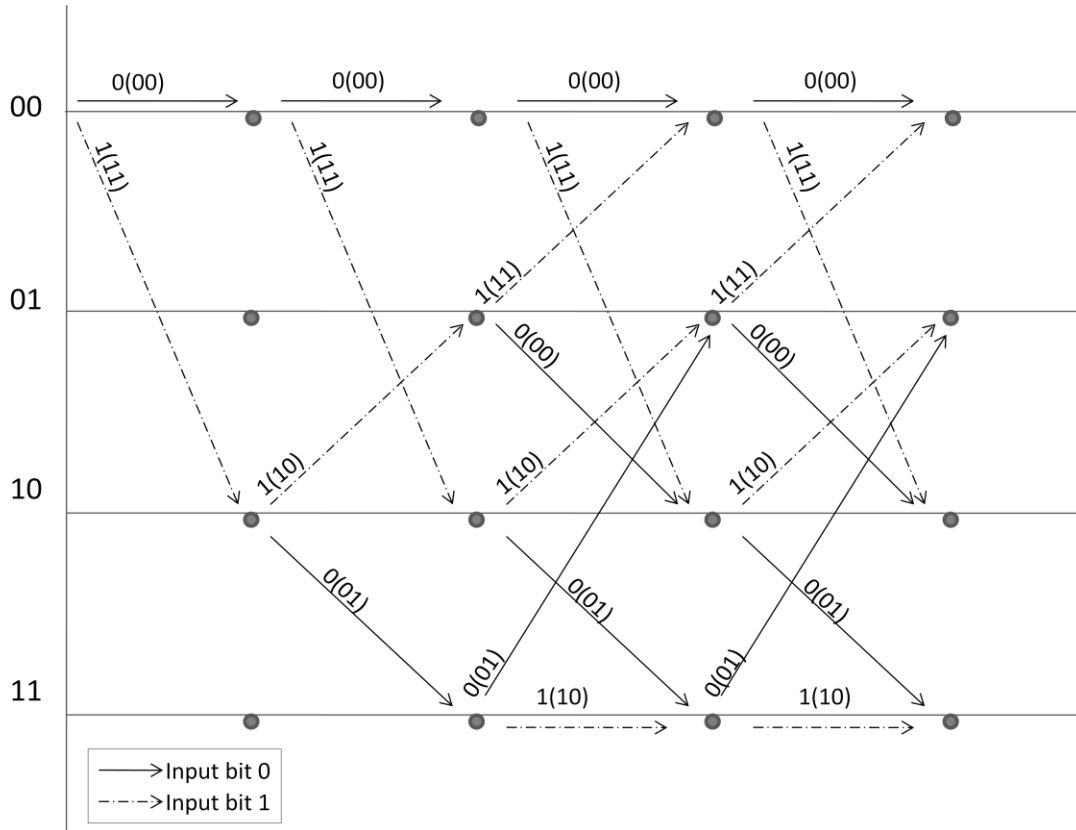
Figure 4.5: Trellis diagram for the convolutional encoder in Fig. 4.3 [45]

4.3.3   Puncturing

The concept of puncturing defines deletion of some bits in the code bit sequence according to a fixed rule which can introduce decrement in the codeword length and increment in the overall code rate. In the originally proposed turbo codes, half of the bits were punctured from each component encoder which provided a coding rate of R = 1/2. Puncturing can provide the advantage of using a single hardware for achieving various coding rates, which can be implemented through software and configured dynamically according to the link characteristics, a flexibility missing if using a fixed scheme.

The most typical alternate for puncturing is simply not to puncture at all, which, if implemented in the original turbo codes would provide a rate of R = 1/3, and might remove some of the obscurities related to puncturing and the proper choice of interleaving and encoding. However, specific schemes with provision of pre-emptive information can allow for the designing of punctured codes which may provide reduction in overhead, also, some of these codes perform nearly as good as general convolutional codes [50].

4.3.4   Interleaving

The convolutional codes can also suffer from distortion due to fading in the channel, therefore it is required to spread out the error bursts with the help of interleaving which has a significant contribution towards elimination of error floor [51]. In block codes, the interleaver stretches out the errors in various codewords, but interleavers in convolutional codes use a different design, they are usually called convolutional interleavers. The encoder output is divided into blocks of length N [45] or multiplexed into expanding buffers from zero to N-1 [52]. The division of coded sequence into N length blocks provides re-ordering of the data within each block, and the increment of interleaver size provides for better coding and decoding performance. While for the other option the interleaver is fed the output sequence from encoder, and it separates them by N-1 other symbols in line, thereby splitting the burst errors.

4.4   Decoding Section

The decoding section of the turbo codes is a comprehensive and complex portion of the complete turbo coding structure where different techniques are implemented for the decoding and correcting of errors if any. On a structural basis, the turbo decoder is completely constructed keeping the encoding section in view, with appropriate components processing the information relevantly. Some of the main attributes and   components   are   discussed   next   to   obtain   a   closer   view   of   the   decoding   section.

4.4.1   Iterative decoding

Turbo codes mainly provide significant benefit from their attribute of building large codes which can be decoded with iterative decoding process among the component decoders.
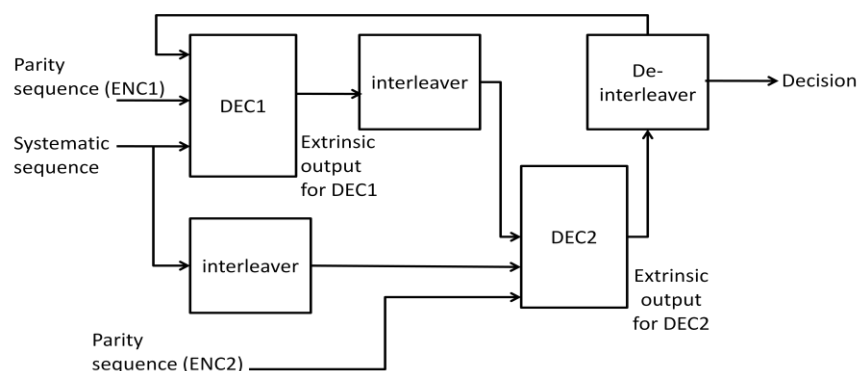
Figure 4.6: A block diagram showing a turbo decoding structure[45]

Associating a component decoder with each of the component encoder for repetitive processing is the basic composition for the 'turbo' in turbo codes, as discussed previously. Interleaving and de-interleaving is performed for transforming the sequence between the code spaces as shown in Figure 4.6.

To decode the *N* sized blocks being input from interleaver, each decoder is involved in the decoding process. The received symbols associated with the first code, parity sequence(ENC1), are decoded at the first decoder (DEC1) which passes a soft information block of length *N* to second decoder. Now the second set of symbols associated with the second code, parity sequence (ENC2), combined with the extrinsic information from first decoder, is decoded by the second decoder (DEC2) and since it has more information, it is expected to execute comparatively better. Also, the information now forwarded from the second decoder to the first decoder might provide better working. This whole process which involves the decoding from both the component decoders is considered as one decoding iteration, while one decoder's operation is referred to as a half-iteration [45].

4.4.2   APP Decoders

The information sharing between the two component decoders allows for better decoding operations, as was discussed above. This information is ideally considered to contain prior knowledge of the probability distribution of each bit in the sequence which brings us to the concept of apriori and aposteriori probabilities. in epistemological terms "apriori" and "aposteriori" are referred to as how, or on what basis, a proposition might be known. Generally, a proposition can be "apriori" perceptible if it is cognizable without dependence on experience, otherwise a proposition can be "aposteriori" perceptible if it is cognizable on the principle of experience [53].

The decoding from the first component decoder and generation of soft information defines the base for aposteriori probability (APP) or soft-output decoder, which forwards the same information to the next decoder, however, this information is used as apriori input for the second component decoder alongwith the second constituent code [45].
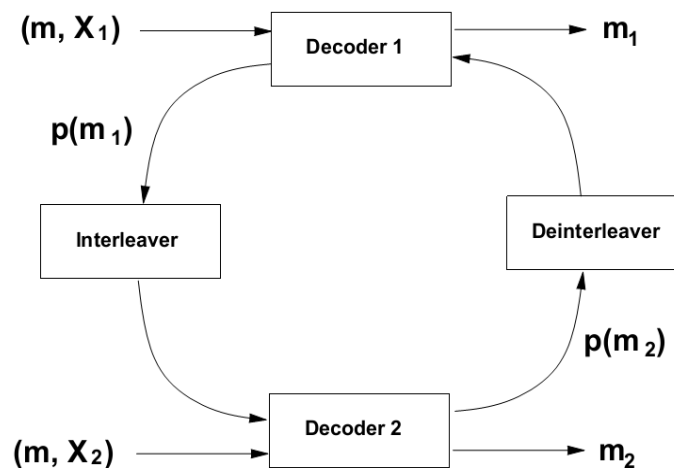
Figure 4.7: A turbo decoder [52]

Figure 4.7 depicts the operation of a turbo decoder section where decoder 1 creates a soft decision in the form of a probability measure *p(m1)* about the information bits transmitted, which is based on the received codeword (m, X1). This reliability information is forwarded to decoder 2, which gives out the probability measure *p(m2)*, generated from its received codeword (m, X2) and the probability measure *p(m1)*.

Then, the information is forwarded to decoder 1 and this time it updates the measure *p(m1)* based on this information and the received original codeword. The information then created is forwarded to decoder 2 and so the process continues for the defined iterations with both the decoders overhauling their probability measures on a rotary basis and eventually agreeing on probability measures that reach hard decisions, m = m1 = m2[52].

4.5   Applications

Convolutional turbo codes have acquired a valuable status in various industrial standards for the past few years with practical implementations already taking place. Some of the codes along with their respective usage domain are listed in Table 4.1.

Table 4.1: Some familiar industrial applications of Convolutional Turbo codes [54]

Application	Turbo Code	Termination	Polynomials	Rates
CCSDS (deep space missions)	Binary,16-state	Tail bits	23, 33, 25, 37	1/6, 1/4, 1/3, 1/2
UMTS, Cdma2000 (3G mobile)	Binary, 8-state	Tail bits	13, 15, 17	1/4, 1/3, 1/2
DVB-RCS (Return Channel over Satellite)	Duo-binary, 8-state	Circular	15, 13	1/3 up to 6/7
DVB-RCT (Return Channel over Terrestrial)	Duo-binary, 16-state	Circular	15, 13	1/2, 3/4
M4 (Inmarsat)	Binary, 16-state	None	23, 35	1/2
Skyplex (Eutelsat)	Duo-binary, 8-state	Circular	15, 13	4/5, 6/7
WiMAX (IEEE 802.16)	Duo-binary, 8-state	Circular	15, 13	1/2 up to 7/8

For the block sizes ranging from short to medium, the relevant scheme for coding is 8-state turbo codes usually used for ARQ systems. While different broadcast systems employing long blocks, or high coding rates typically prefer 16-state turbo codes. Currently, research is being carried out on several

complications to reduce the number of iterations and to simplify the decoder section in turbo codes [54].

4.6   Simulation model

The turbo coding and decoding was simulated independently with Matlab and Simulink before it was integrated to the RoF system model, as would be discussed in the following chapter. The simulation model for the turbo code is shown in Figure 4.8.
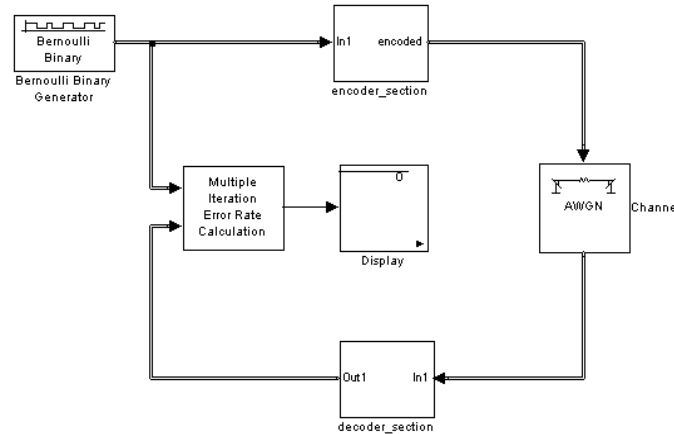
Figure 4.8: A Simulink model for Turbo coding and decoding

The source used for the binary sequence generation is a bernoulli binary generator with a probability of 0.5 for a zero in the generated sequence, the encoder section performs the data coding and the additive white gaussian noise (AWGN) channel is used to emulate the transmission channel. The transmitted sequence is then decoded in the decoder section while the error rate is calculated with respect to the original sequence.

The encoder section is composed of a pair of convolutional encoders combined together in parallel with the second encoder preceded by an interleaver. The systematic and recursive bits are combined according to the 1/3 code rate and after wards sent to interleaver and converted before being sent on the channel as shown in Figure 4.9. The code rate can also be changed by puncturing the sequence before conversion.
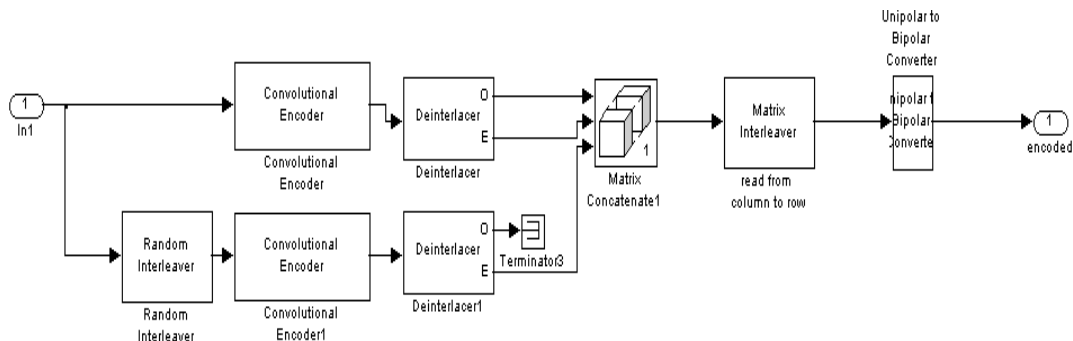
Figure 4.9: Encoder section of the turbo code simulation model

The decoder section is composed of the initial data processing block which extracts and provides the relevant data from the sequence to the APP decoder pairs arranged in a cyclic order with interleaving and de-interleaving taking place between the information transfers before being sent for decision making as shown in Figure 4.10.
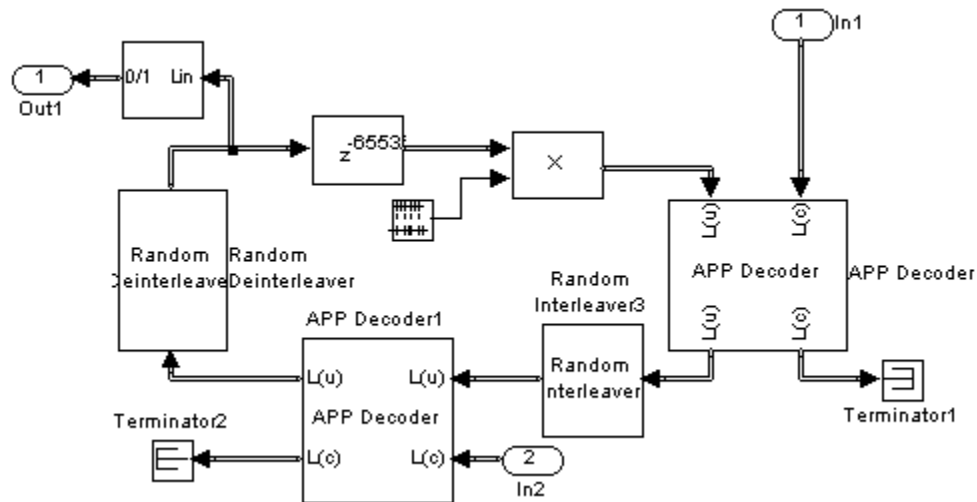
Figure 4.10: Decoder section of the turbo code simulation model

The graphs for the bit error rate (BER) against the signal to noise ratio are useful for defining the performance of the codes, the graphs shown in Figure 4.11 and Figure 4.12 depict the BER for the specified number of decoder iterations for the 1/2 and 1/3 code rates respectively.
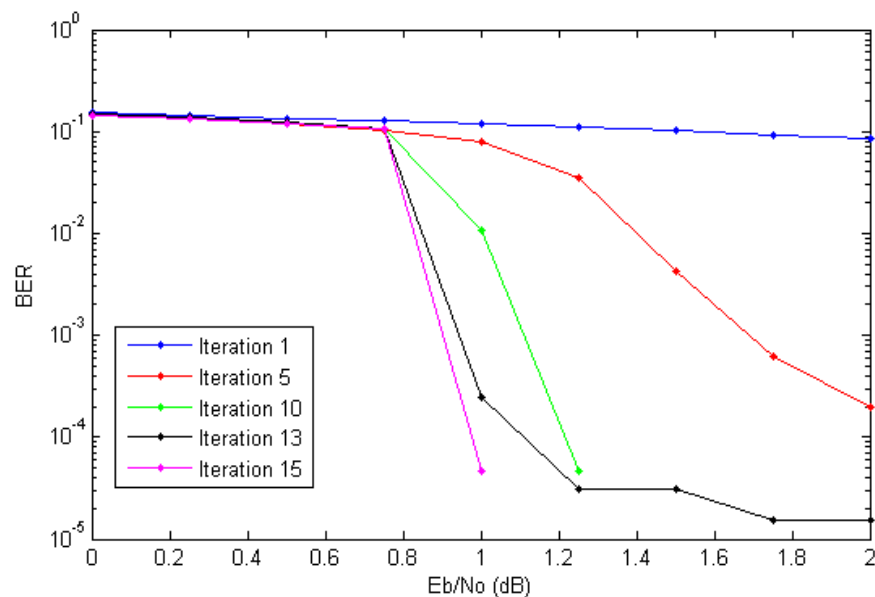
Figure 4.11: A graph showing the turbo decoder performance for Rate=1/2, Constraint length=5 and data bits=2^{16}

The iterative decoding procedure provides a less cumbersome method to correct the error in data, but the codes display an error floor which can be difficult for systems requiring very low BER, as analyzable in Figure 4.11 the error floor occurs at about 10^{-5}, while the 10th decoding iteration (green curve) reaches zero error at 1.25 dB and the 15th decoding iteration (pink curve) at 1dB value of signal to noise ratio.
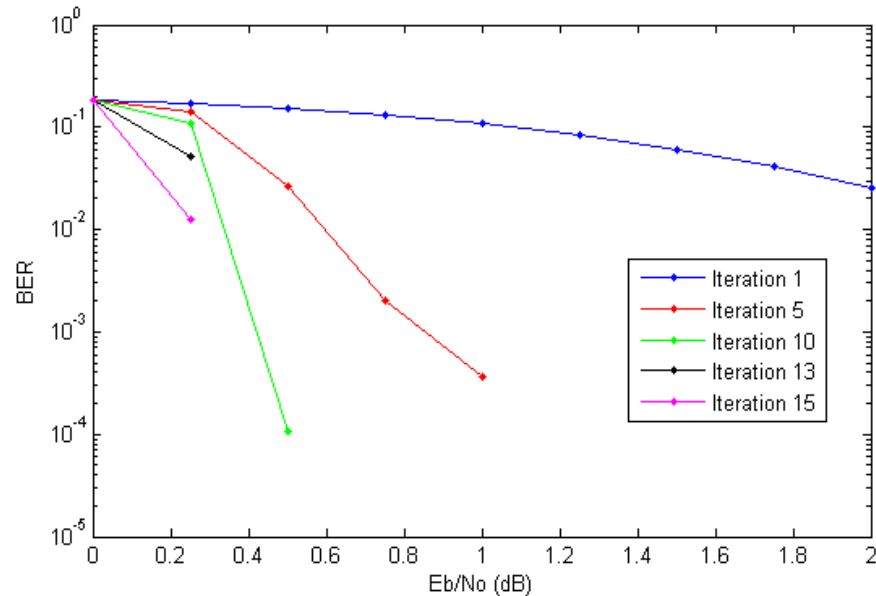
Figure 4.12: A graph showing the turbo decoder performance for Rate=1/3, Constraint length=5 and data bits=2^{16}

The (2^{16} = 65536) bits long sequence of data was coded in both the code rates, where 1/3 code rate provided higher redundancy than the 1/2 code rate; at lower signal to noise ratios, with BER values of about 10^{-4} for a signal to noise ratio of 0.5 dB for the 10th iteration.

The turbo codes are used in the study along with the OFDM scheme for the improvement of optical receiver sensitivity by mitigating the unbalanced noise distribution in subcarrier signals [55] and also because they can enhance the BER [56]. The turbo codes can compensate for the signal fading and can provide the laser communication systems to achieve lower BER than conventional encoding/decoding methods [57]. However, for the turbo decoder to perform optimally, accurate noise statistics for the optical fiber transmission are vital for utilization in the decoding algorithm [58].

5 Simulation Results and Performance Analysis

5.1 Introduction

The platform used for the simulative analysis and the composition of the RoF system model in the simulation platform is described in the current chapter in detail along with the individual results for different components and the analysis of complete system's simulation results.

The chapter begins with introduction to the optical simulation softwares significant to the industry and an explanation of the Optisystem software used in this study. The integration of Matlab with optisystem is also discussed since the error correction procedures are implemented outside the optical simulator.

5.2 Optical Simulation Software

Optical communication technologies require high performance components and extensive testing for their practical implementation, but for some cases like long-haul and submarine systems, the tests and experiments carried out in laboratories usually become costly. This is where numerical simulations provide a low cost solution with their expansive capabilities of advanced input signal modulation formats, realistic noise and dispersion emulation for optical fiber, polarization effects and other features relating to the practical implementation of the systems can be easily carried out with these simulators. Currently there are many optical simulators being utilized by the industry and institutions for research and testing purposes with many of them focusing specific domains related to the optical technology, however some main stream commercial simulation softwares are listed below [59].

- VPItransmissionMaker[TM] WDM, a commercial software sold by VPIsystems. VPItransmissionMaker[TM] WDM is a tool for the design of new photonic systems including link and all-optical networks [59].

- RSoft OptSim, a commercial software sold by RSoft. OptSim provides a modeling and simulation environment supporting the design and performance evaluation of the transmission level of optical communication systems [59].

- OptiSystem, a commercial software sold by by Optiwave. OptiSystem is optical communication system and amplifier design software that enables users to plan, test, and simulate almost every type of optical link in the transmission layer of a broad spectrum of optical networks[59].

Different examples of the systems and networks are added as samples in the OptiSystem library, the users can also construct designs relating to the following domains [60]:

- Next Generation optical networks
- Optical networks currently in industrial use
- SONET/SDH ring networks

- Amplifiers, receivers, transmitters etc.

The OptiSystem software offers the facility of transportation of data to and from various other platforms including Matlab, Simulink and Agilent softwares among others. This accessibility between Matlab and OptiSystem allows for data processing and mathematical operations to be performed in a simplified way.

5.3   OptiSystem Model Layout

The project layout is the main working area where components are laid out by drag and drop action, and connected, and also editing can be done. A wide range of components are available in OptiSystem's large component library section. The global parameters can be configured by double clicking the main layout while the component parameters can be changed by performing the same action on the required component. The results can be viewed by opening the visualizers after performing the calculation of the project.
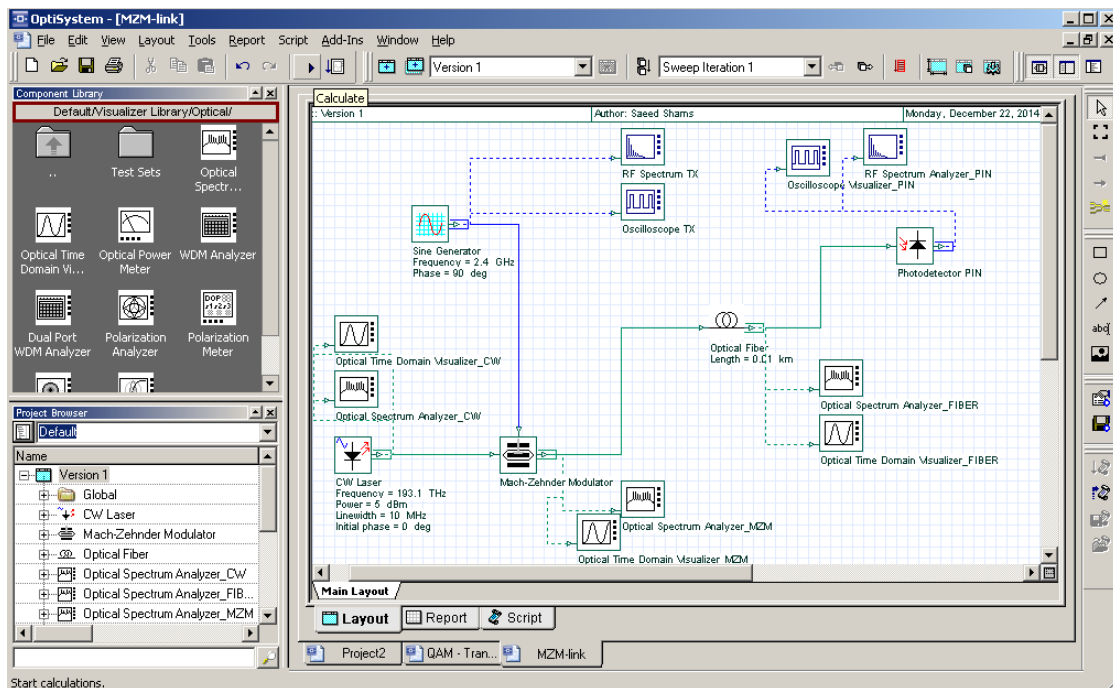
Figure 5.1: A project layout window for the OptiSystem software

A project layout for OptiSystem is shown in Figure 5.1, the column to the left of project layout shows the component library and the project browser sections while calculation of the project can be carried out from the drop down File menu and then selecting calculate or from the push button just above the project layout.

5.4   Back-to-back OFDM System Model

Before defining the RoF model, the back to back OFDM model is explained because it is helpful in the understanding of the data processing operations taking place at the transmitter and receiver sections of the RoF system. The OFDM modulator and demodulator components are connected to each other facing in opposite directions while the QAM sequence generator and decoder are respectively connected before the OFDM modem as shown in Figure 5.2. The number of bits per symbol parameter is defined in the QAM codec while the number of subcarriers and other related parameters are configured from OFDM modem operations, the components are described individually in the following sections.
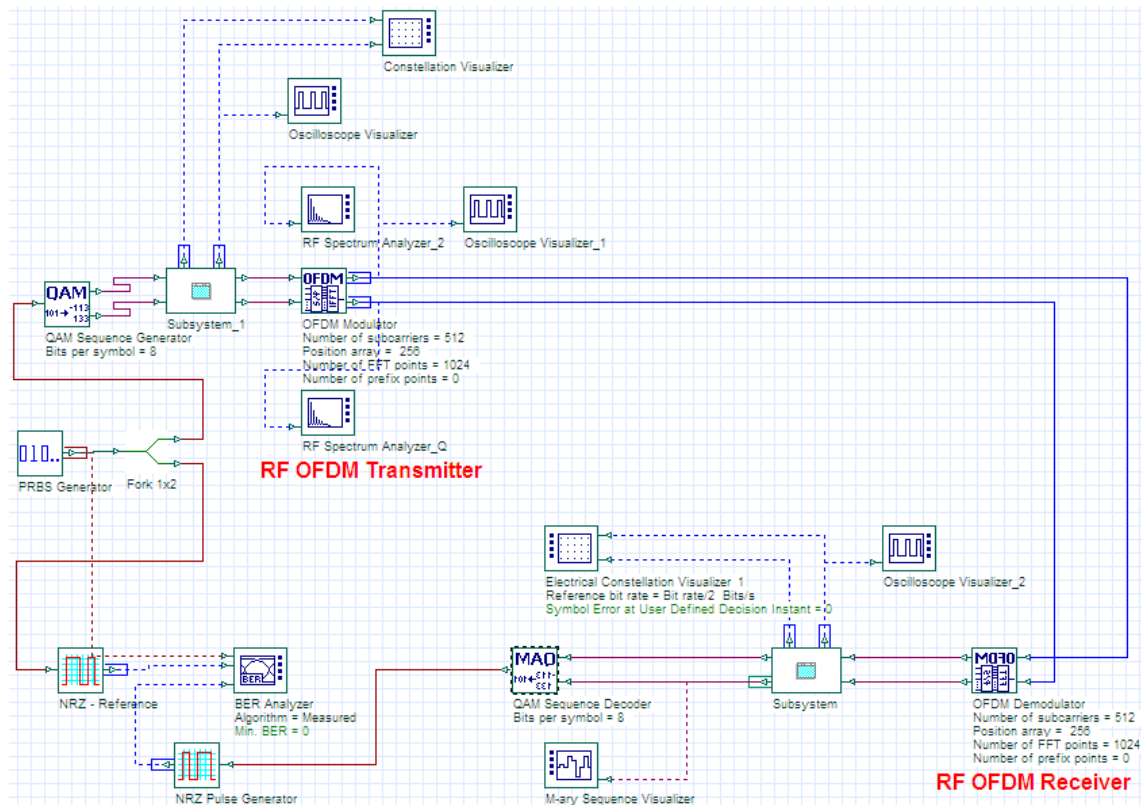
Figure 5.2: A layout showing back-to-back OFDM communication link

The global parameters for the layout are configured as defined in Table 5.1. The parameters for different components are described with their respective variations applied for calculation of results.

Table 5.1 Global parameters configuration.

Name	Value	Units
Bit rate	10e+009	Bits/s
Time window	1.6384e-006	S
Sample rate	40e+009	Hz
Sequence length	16384	Bits
Samples per bit	4	
Number of samples	65536	

5.4.1   QAM Sequence Generator Block

A basic component of the RoF system, the mapping of data to symbols is carried out by digital modulators. For this study, QAM is used. The incoming train of bits is divided into two parallel subsequences with the QAM sequence generator. With a serial to parallel conversion, these can be transmitted in two i.e. in-phase and quadrature carriers and the amplitude can be varied with relevance to the source symbols. For each output port, the amplitude takes one of the values from the set of available amplitudes.

The set of amplitudes for each output port are defined in the Optisystem help menu for the component as,

$$a = (2i - 1 - M) \tag{5.1}$$

where, $i = 1, 2, ..., M$

and M is the number of binary sequences defined by:

$$M = 2^{h/2} \tag{5.2}$$

where, h is the number of bits per symbol.

The QAM set is defined by the square of M. If $h = 6$, $M = 8$, then we have a 64-QAM signal, and for the 16-QAM signal we have $h = 4$, $M = 4$. Figure 5.3 shows the constellations obtained at the constellation visualizer before the OFDM Transmitter, for both the signals.

Figure 5.3: A set of constellation diagrams showing (a) 64-QAM and (b) 16-QAM signals plotted in Optisystem's Constellation Visualizer component

5.4.2 OFDM Modulator Block

The orthogonal frequency division multiplexing (OFDM) distributes the data symbols on different frequency subcarriers orthogonal to each other, before multiplexing them together. Usually digital modulation formats like BPSK, QPSK, QAM etc. are app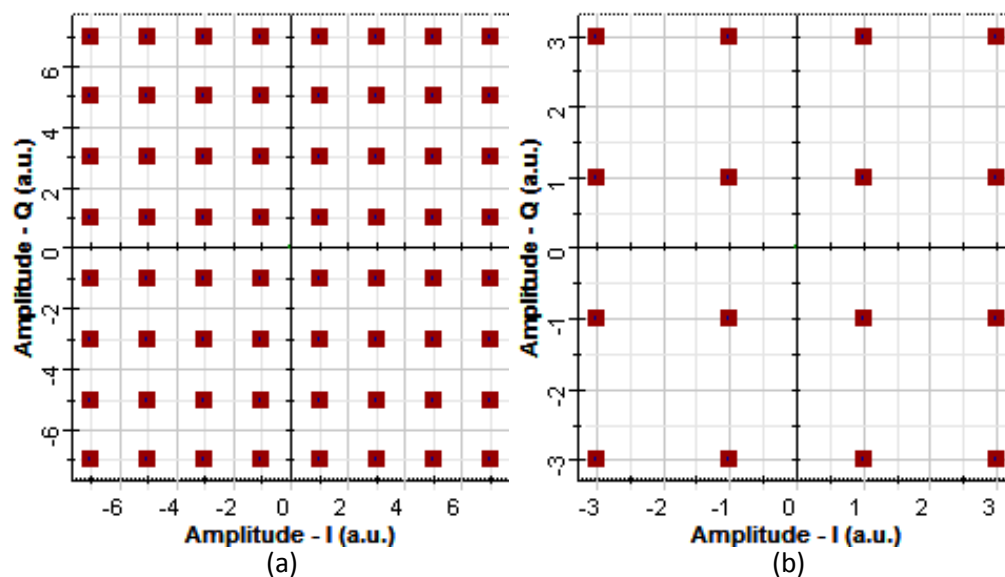lied to create symbol sequence which is divided in parallel and each symbol is assigned to a lower rate data stream by the OFDM. The OFDM Modulator available in OptiSystem is composed of different blocks as shown in Figure 5.4.
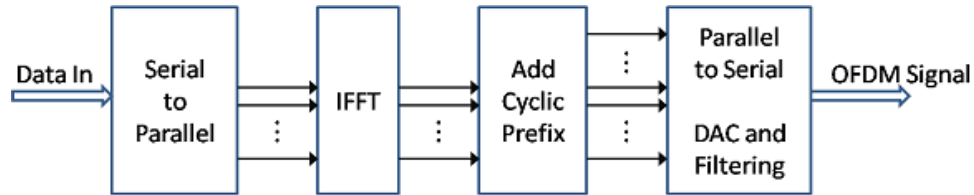
Figure 5.4: A diagram depicting the different parts of an OFDM Modulator component [60]

The spectrum is mapped with the incoming sequence of symbols converted from serial to parallel, afterwards an inverse fourier transform is used to find the corresponding time waveform. The cyclic prefix i.e. guard period can then be added to start each symbol. There exists an option of a cyclic extension of the symbol transmitted or a guard time with zero transmission in the component. Different interpolation techniques like step, linear, and cubic can be used to function as the DAC. After the DAC, the parallel data is shifted back into the serial symbol stream.

The OptiSystem's OFDM modulator places the subcarriers on the frequency bins allocated within the spectrum by the IFFT processing of the data sequence, the spectrum is calculated from

This spectrum is spread equally in the positive and negative frequencies with the initial subcarriers getting placed in the negative frequency bins, unless the 'user specified position' option is used to position the subcarriers in the spectrum. The difference between the frequency bins or subcarrier frequencies are calculated by the following relations,

$$T_b = 1/bit\ rate \tag{5.3}$$

where,
T_b is the bit period

The symbol period for the modulated data (QAM) can be found by:

$$T_m = h * T_b \tag{5.4}$$

where,
T_m is the symbol period for the QAM modulated data
h is the number of bits per symbol.

Now, the OFDM symbol period can be found by multiplying the number of subcarriers with T_m. One OFDM symbol is composed of a parallel distributed column of QAM symbols, in the subcarriers.

$$T_{sym} = N * T_m \qquad (5.5)$$

where,

T_{sym} is the OFDM symbol period

N is the number of subcarriers

The subcarrier frequencies are integral multiples of the subcarrier frequency difference or (1/T$_{symbol}$), where T$_{symbol}$ is the symbol period as defined in the Optisystem help menu for the OFDM modulator. The frequency difference for the subcarriers is the inverse of the OFDM symbol period

$$\Delta f = 1/T_{sym} \qquad (5.6)$$

where,

Δf is the frequency difference between the subcarriers

The back to back OFDM link as defined in Figure 5.2, is analyzed for the different number of subcarriers and the readings noted for 6 bits per symbol (64 QAM) with a 32-point FFT utilizing 16 of the subcarrier frequencies and an initial spectrum position of 8. From the relations discussed above, frequency difference between the subcarriers is calculated as 104.16 MHz.

Therefore a bandwidth of 1.666 GHz is provided by the 16 subcarriers. The frequency difference and the span of subcarriers and FFT bins is verifiable from the OFDM modulator's graph available from the optisystem's project browser window.

For an increased number of subcarriers the frequency difference between the subcarriers decreases in the same proportion with 256 subcarriers having a spacing of 6.51MHz and for 512 subcarriers, the frequency spacing between carriers is decreased to 3.255 MHz and the bandwidth is further filled up as shown in the RF Spectrum Analyzer (RFSA) graphs for the I (red curve) and Q (black curve) components combined for 512 subcarriers in Figure 5.5.
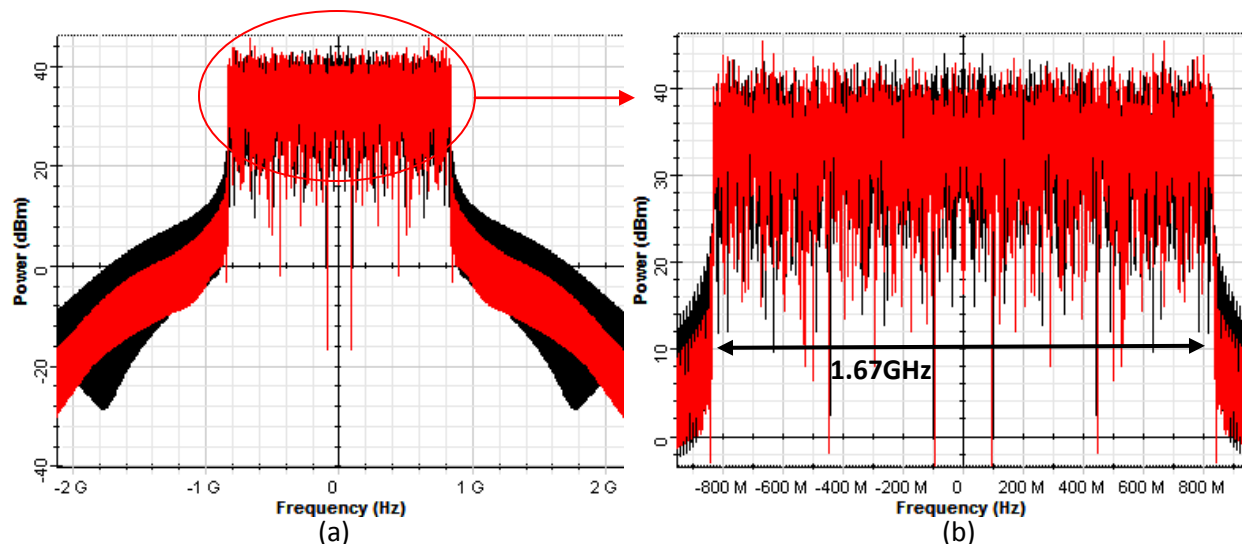

Figure 5.5: (a) A combined plot for I and Q components for the 64-QAM, 512 subcarrier OFDM (b) Zoomed in view of the subcarriers bandwidth

As we can observe, the bandwidth is about 1.67GHz and a power of about 40dBm for both the components. The calculated bandwidth for the different subcarriers is verified by measuring the I and Q component's RFSA outputs of the OFDM modulator (see Figure 5.9). The readings are listed in Table 5.2.

Table 5.2: The bandwidth and peak power measurements of 64-QAM and 16-QAM OFDM signals for different subcarriers

Number of Subcarriers	64 QAM				16 QAM			
	I - component		Q - component		I - component		Q - component	
	Bandwidth (Hz)	Peak power (dBm)	Bandwidth (Hz)	Peak power (dBm)	Bandwidth (Hz)	Peak power (dBm)	Bandwidth (Hz)	Peak power (dBm)
16	1.86e9	29.82	1.83e9	29.88	1.34e9	26.71	1.35e9	25.05
32	1.76e9	32.085	1.76e9	34.2	1.3e9	27.39	1.3e9	28.47
64	1.68e9	36.38	1.71e9	34.862	1.27e9	31.34	1.26e9	31.46
128	1.68e9	37.65	1.67e9	38.8	1.26e9	33.99	1.25e9	33.96
256	1.68e9	41.21	1.67e9	40.93	1.25e9	36.72	1.25e9	36.7
512	1.67e9	45.5	1.67e9	43.96	1.25e9	40.35	1.25e9	39.9

The OFDM signals were passed through low pass cosine roll off filters to minimize the excess portion of the signal and bring it within the acceptable 7.5 GHz range. The 64-QAM and 512 subcarrier OFDM signal is filtered and the RFSA output for the I component is shown in Figure 5.6, where the bandwidths of signal and subcarriers are measured to be 6.6 GHz and 837 MHz respectively.
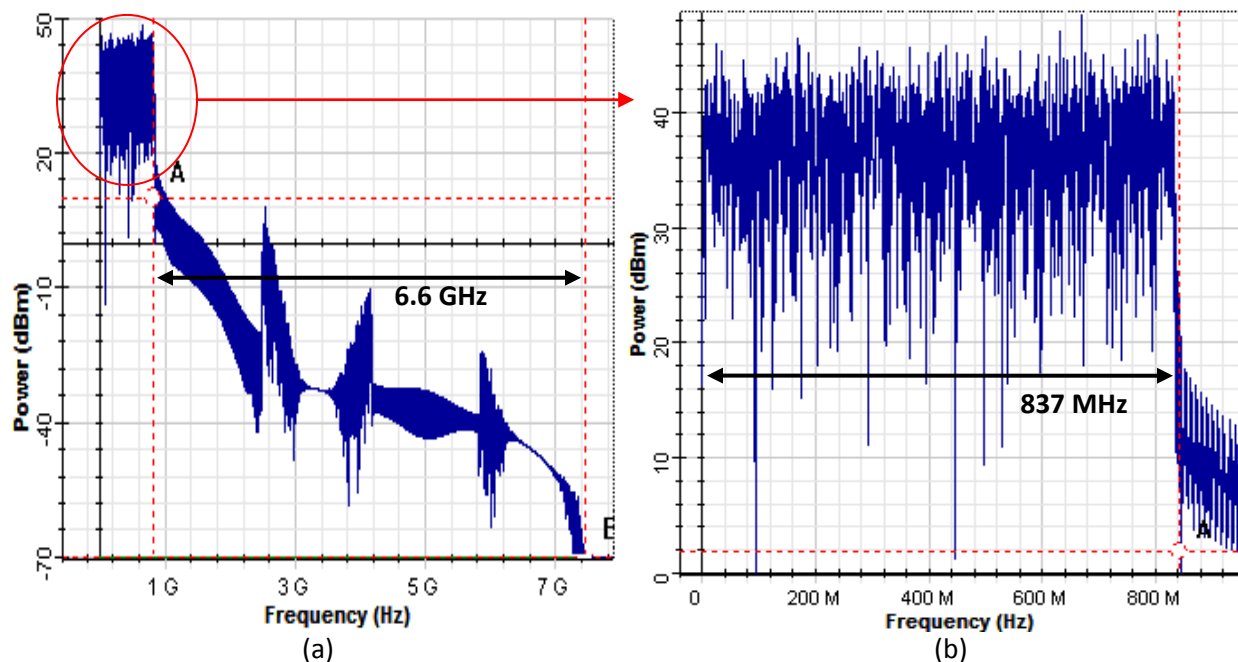

Figure 5.6: (a) Low-pass filter RFSA plot for I component for the 64-QAM, 512 subcarrier OFDM (b) Zoomed in view of the subcarriers bandwidth

5.4.3   Quadrature Modulator Block

The translation of an OFDM signal to the radio frequency and the up-conversion procedures are carried out with the quadrature modulator component available in the electrical modulator section of the transmitters' library in OptiSystem. The I and Q input electrical signals are multiplied with cosine and sine carriers according to the frequency, gain and phase values provided by the user. The output signal is modulated according to the following relation,

$$v_{out}(t) = G[I(t)\cos(2\pi f_c t + \phi_c) - Q(t)\sin(2\pi f_c t + \phi_c)] + b \tag{5.7}$$

where,

I and Q are the input electrical signals

and the configurable parameters are,

ϕ_c is the phase of carrier,

f_c is the carrier frequency,

G is the parameter gain and

b is the bias.

The I and Q mixed channel is depicted in Figure 5.7 with 20 MHz resolution bandwidth, which shows a total bandwidth of 15 GHz while the bandwidth of the subcarriers is measured to be 1.69 GHz with the center frequency of 7.5 GHz.
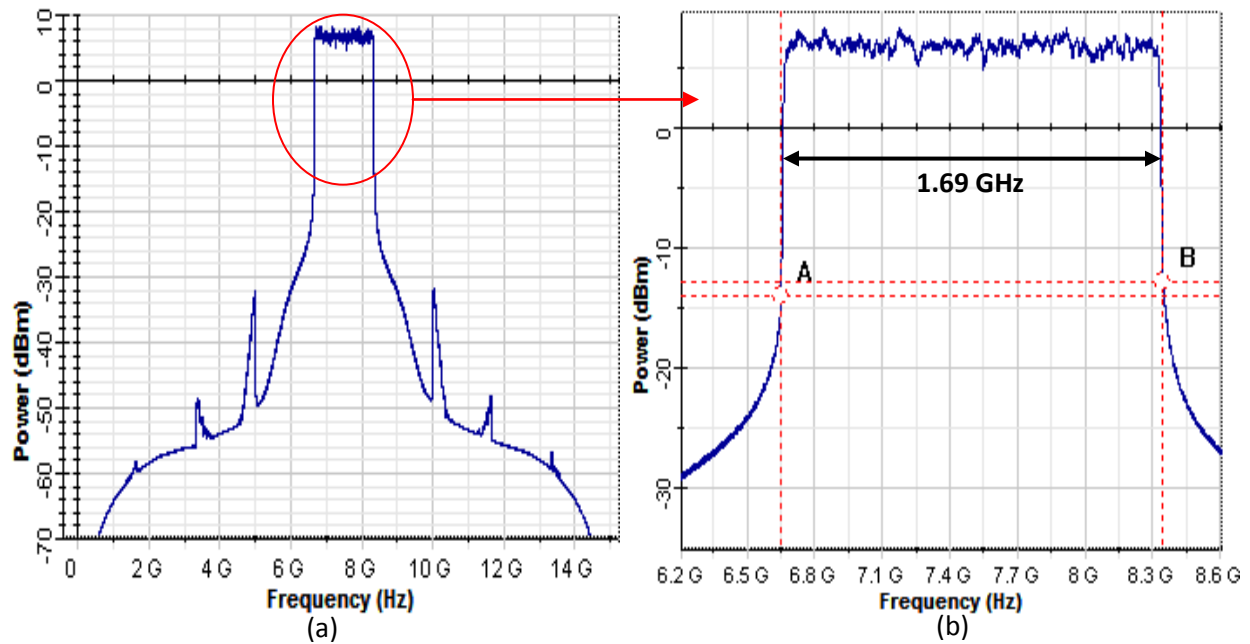
Figure 5.7: (a) Quadrature modulator RFSA output for 64 QAM and 512 subcarrier OFDM signal up-converted to 7.5 GHz (b) Zoomed in view of the subcarriers and their bandwidth

5.5   RoF System Simulation Model

The complete simulation model of the RoF system consists of three main segments which are the transmission section, the optical transmission link section and the receiver section. The optical

transmission link and receiver section is defined briefly in the paragraphs ahead, before that a closer view of the transmission section is given. The complete RoF system layout is depicted in the Figure 5.8.
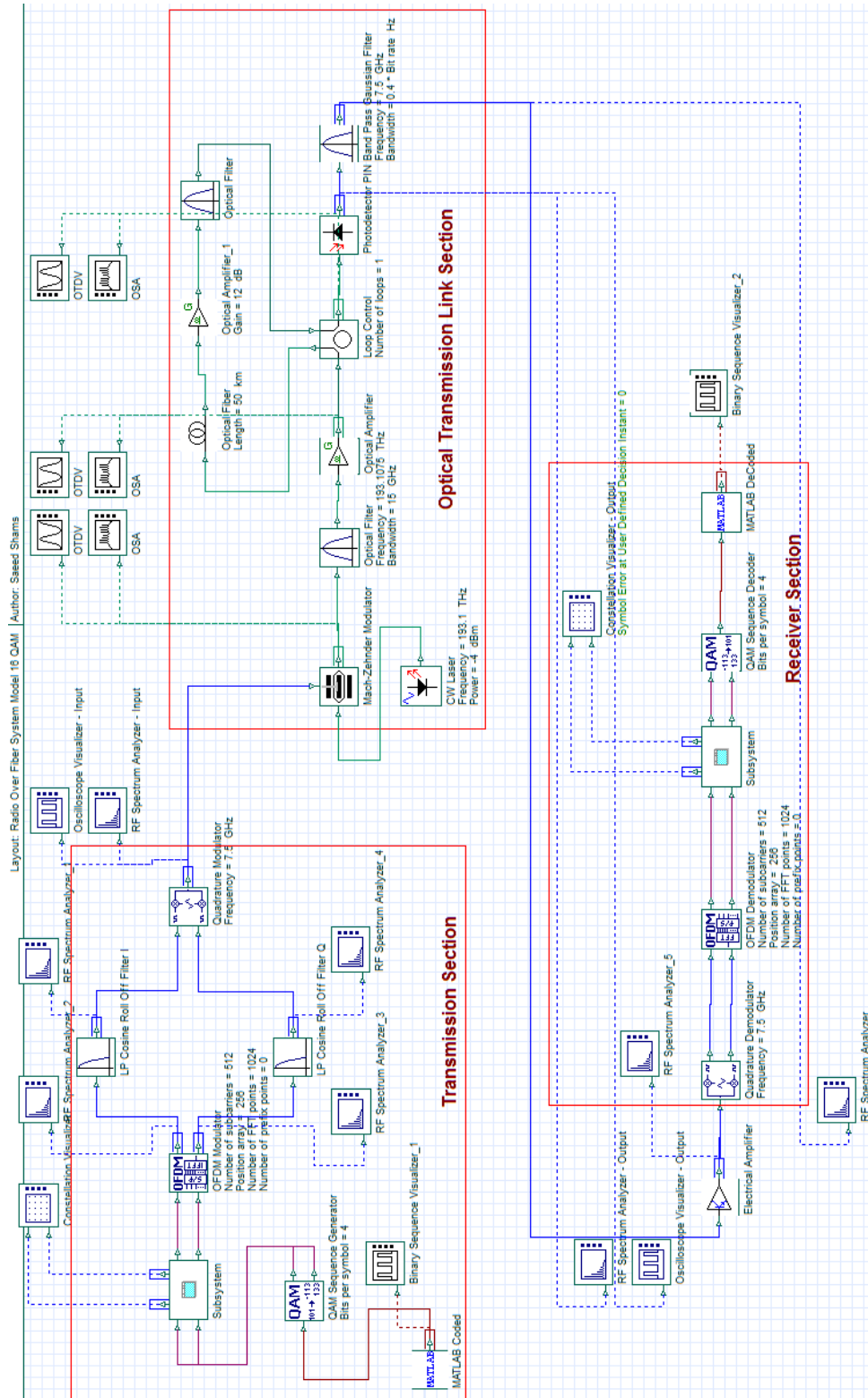
Figure 5.8: The RoF system layout in Optisystem

5.5.1 The Transmission Section
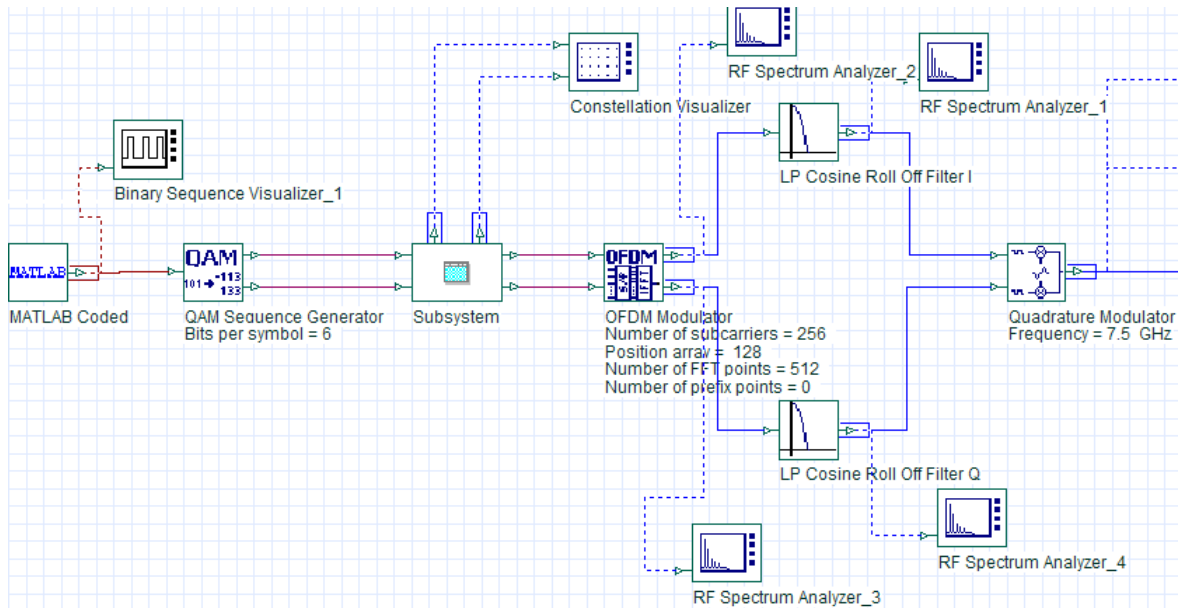
Figure 5.9: The transmission section of the RoF system

The Figure 5.9 describes the transmission section of the RoF simulation model where coded data from Matlab is input through the Matlab component and modulated by the QAM sequence generator component and the OFDM modulator performs the distribution of data among the subcarriers and IQ mixing is carried out by the quadrature modulator component.

5.5.2 The Optical Transmission Link Section

The optical transmission link is a critical section of the whole RoF model as the data integrity has to be ensured through this very part of the system. For long range transmissions appropriate configurations are required for better received signals. The externally modulated optical source is shown in Figure 5.10.
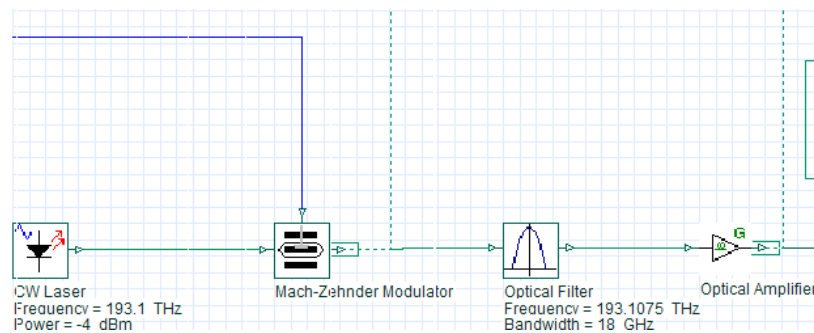
Figure 5.10: Externally modulated optical source for the optical transmission link

The modulated data from the quadrature modulator is provided to the MZM, with a default extinction ratio of 30dB, it modulates the CW light signals from the CW laser component set to -4dBm power and an emission frequency of 193.1 THz (1552.5nm). The optical filter is used for the same frequency window along with an amplifier providing a gain of 13dBm before being sent on to the fiber. The Optical Spectrum Analyzer (OSA) output for the MZM is depicted in Figure 5.11 with resolution bandwidth of 0.001nm.
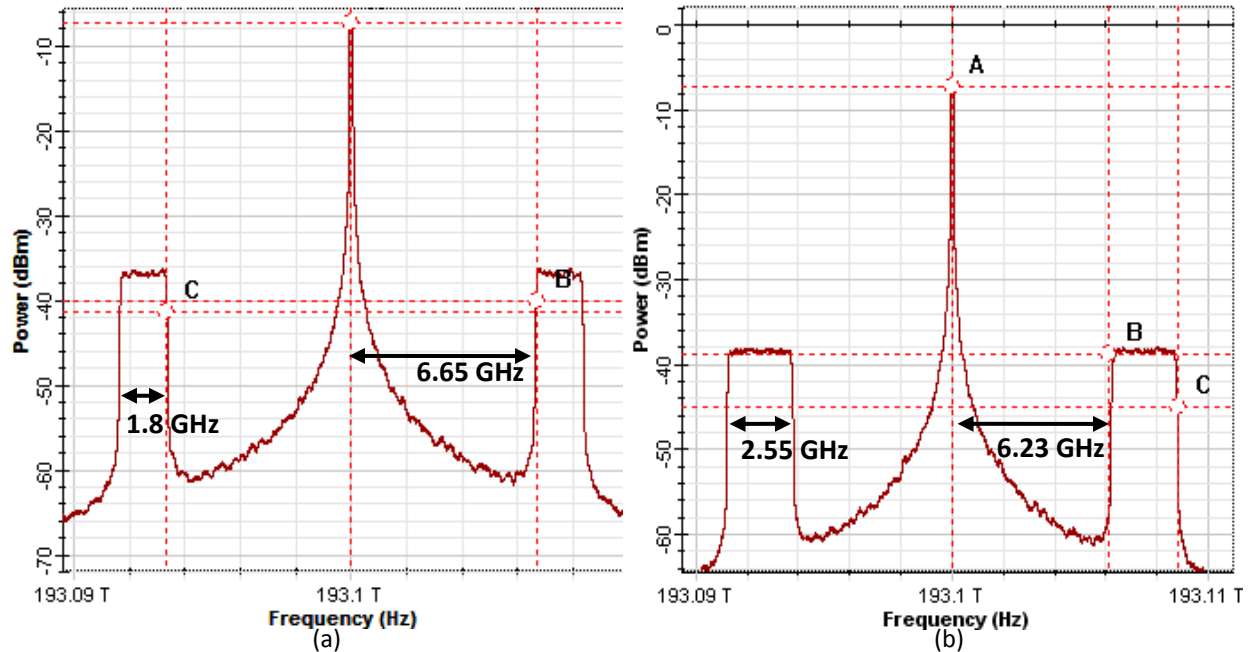
Figure 5.11: OSA output of MZM for (a) 64-QAM (b) 16-QAM and 512 subcarrier OFDM signal

The sidebands' width was measured to be around 1.8 GHz and was placed at a distance of 6.65 GHz from the central optical frequency of 193.1 THz, as shown in Figure 5.11

The CW laser component is used for the generation of optical signals with reference to the Power defined by the user and having waveform of continuous nature. It provides a fixed amplitude signal to the Mach-Zehnder modulator (MZM), an intensity modulator based on an interferometric principle. It changes the optical power level of the light but preserves the amplitude; it consists of two 3 dB couplers which are connected by two waveguides of equal length (see Figure 5.12).
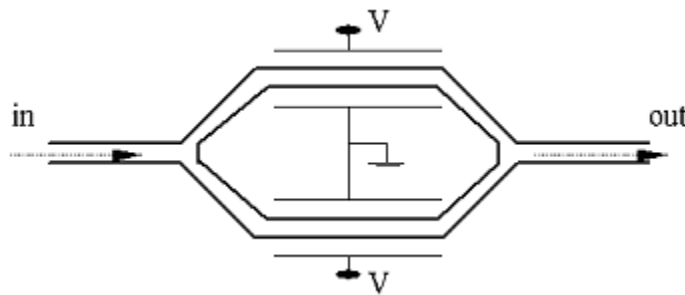
Figure 5.12: A MZM schematic[16]

By means of an electro-optic effect, an externally applied voltage can be used to vary the refractive indices in the waveguide branches. The different paths can lead to constructive and destructive interference at the output, depending on the applied voltage. Then the output intensity can be modulated according to the voltage.
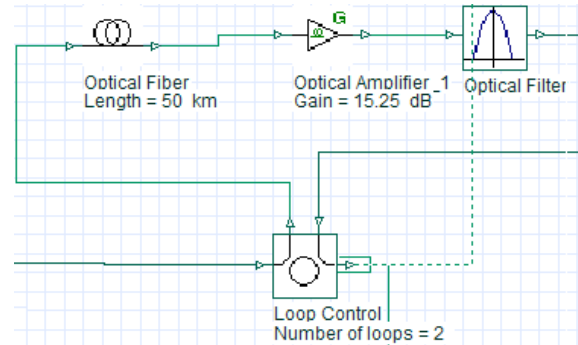
Figure 5.13: Optical fiber link in the optical transmission

The optical fiber link consists of an optical fiber component, an optical amplifier and an optical filter along with the loop control for varying the fiber transmission spans, as shown in Figure 5.17. The optical fiber link is implemented in 50 km spans with an attenuation of 0.2 dB/km and a dispersion value of 16.75 ps/nm/km. An optical amplifier with 15.25 dB gain value amplifies the output and an optical filter with the 193.1 THz window is used. The optical fiber component simulates the propagation of an optical field in a single-mode fiber with the dispersive and nonlinear effects taken into account by a direct numerical integration of the modified nonlinear Schrödinger (NLS) equation (when the scalar case is considered) and a system of two, coupled NLS equations when the polarization state of the signal is arbitrary. The optical sampled signals reside in a single frequency band, hence the name total field. The parameterized signals and noise bins are only attenuated. The OSA outputs after the fiber link are shown in Figure 5.14 for the 16-QAM and 64-QAM schemes for the different fiber lengths.
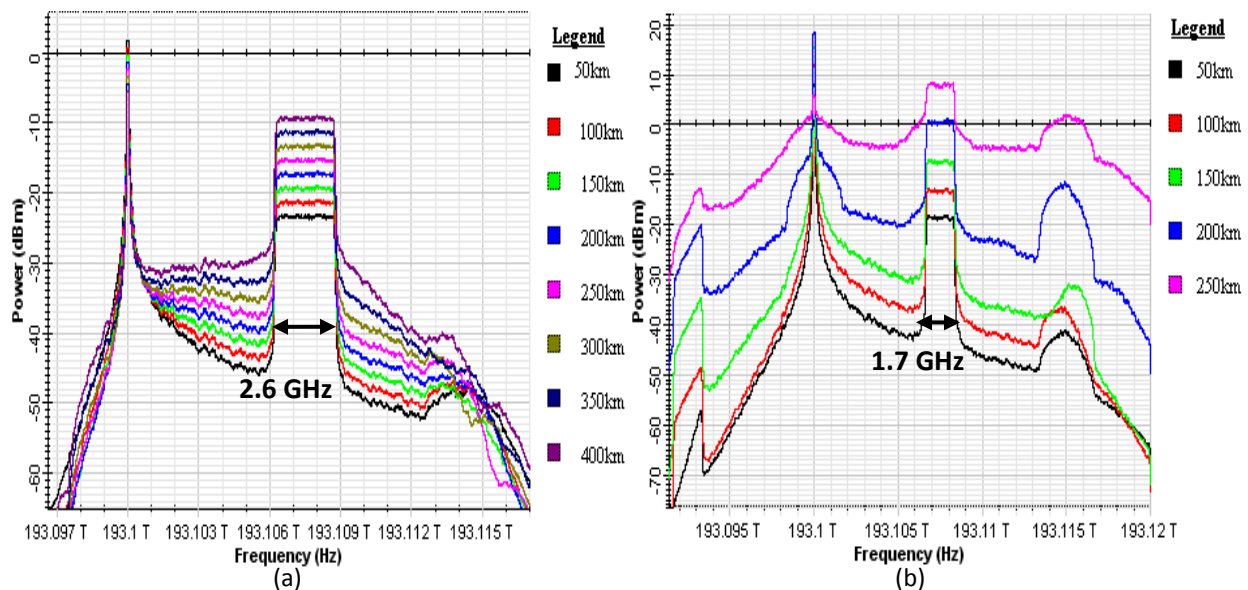
Figure 5.14: OSA output of the optical fiber for various fiber lengths using (a) 16-QAM (b) 64-QAM and 512 subcarriers

The measurements for the signal to noise ratio (SNR) for the optical fiber output were done for the different fiber lengths implementing the 16-QAM and 64-QAM schemes for the 512 subcarriers. The table lists the readings that were observed.

Table 5.3: SNR readings for the optical fiber output for different fiber lengths with 16-QAM and 64-QAM

| Fiber Length (Km)	16-QAM SNR(dB)	64-QAM SNR(dB)
50	58.545	48.2083
100	65.247	56.254
150	67.3	62.883
200	69.308	71.096
250	71.318	78.485
300	73.318	-
350	75.308	-
400	77.308	-

The PIN PD is the receiver and converter of optical signals to electrical as shown in figure 5.15.
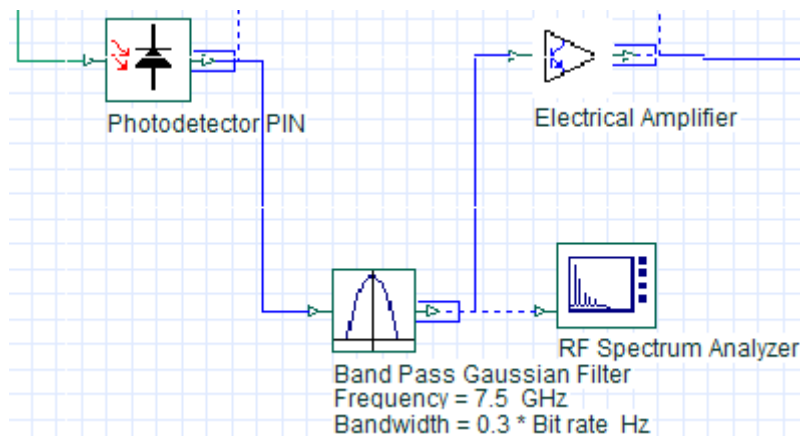
Figure 5.15: Optical receiver for the optical transmission link

The PIN PD component of Optisystem filters the incoming optical signal and noise bins are filtered by an ideal rectangle filter to reduce the number of samples in the electrical signal. The parameter *Sample rate* defines the new sample rate, while the option of *Noise calculation type* can define the combination or separation of the noise with the signal. The sensitivity of a receiver can be defined by optimizing the receiver parameters like optimizing the thermal noise in receiver, to obtain a specific BER.

The RFSA outputs for the received signal at the photodiode are shown in Figure 5.16 for the 16-QAM and 64-QAM schemes using 512 subcarriers, defined for the different fiber lengths, the bandwidths appear to be approximately the same as the transmitted signal as defined previously in Table 5.2.
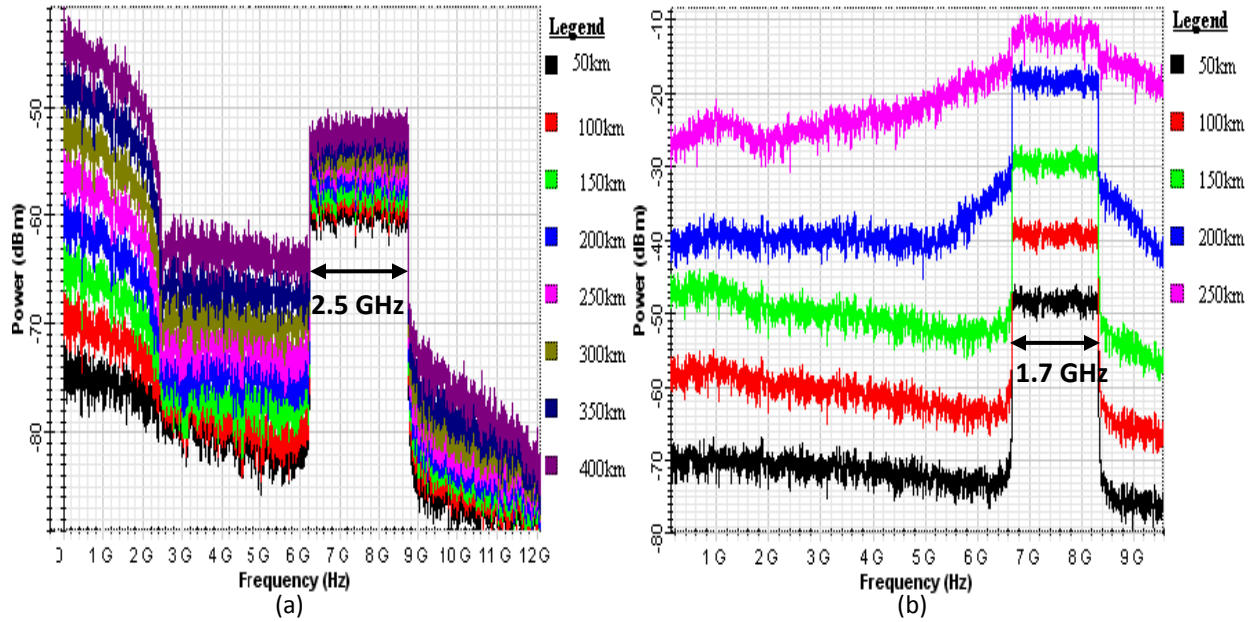
Figure 5.16: RFSA output of the photodiode over different fiber lengths for (a) 16-QAM (b) 64-QAM schemes and 512 subcarriers

The measurements for the signal to noise ratio (SNR) for the received signal at the photo diode were done for the different fiber lengths implementing the 16-QAM and 64-QAM schemes for the 512 subcarriers. The table lists the readings that were observed.

Table 5.4: SNR readings for the PD output for different fiber lengths with 16-QAM and 64-QAM using 512 subcarriers

Fiber Length (Km)	16-QAM	64-QAM
	SNR(dB)	SNR(dB)
50	-42.76402	-53.93
100	-43.69	-61.84
150	-44.62	-67.74
200	-45.8	-75.783
250	-46.81	-79.736
300	-47.73	-
350	-48.92	-
400	-49.95	-

The band-pass gaussian filter is used to filter the noise added from the fiber propagation and also because of the real and imaginary components of OFDM signal exhibit gaussian distribution [33]. The frequency is configured that of the radio signal transmitted i.e 7.5GHz with a bandwidth of 3GHz. An electrical amplifier adds 16dB of gain to the signal before it is forwarded to the receiver section. The RFSA outputs for the band-pass Gaussian filter shown in Figure 5.17 depict the gaussian response of the filter with bandwidths of 2.5 and 1.7GHz for 16 and 64 QAM respectively.
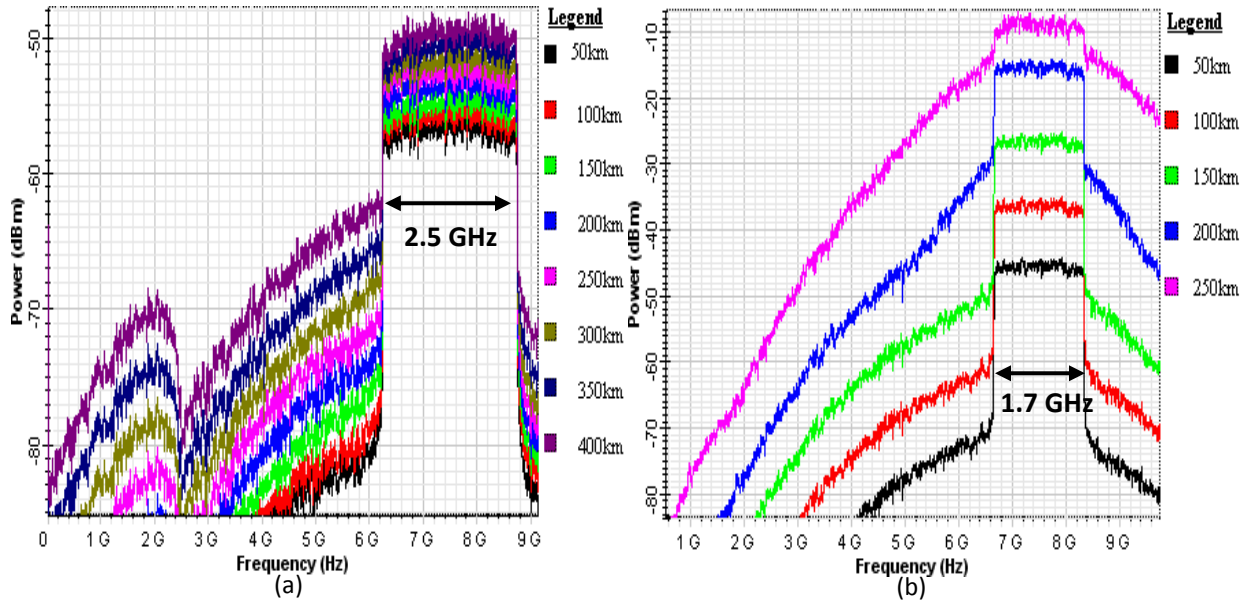
Figure 5.17: RFSA output of the band-pass Gaussian filter for different fiber lengths for (a) 16-QAM (b) 64-QAM schemes and 512 subcarriers

5.5.3   The Receiver Section

The Figure 5.18 shows the final section of the RoF model, the receiver section, which is essentially the reverse implementation of the transmission section. The parameter configurations for the components are also kept equal except for the quadrature modulator, which will be described in the following section.
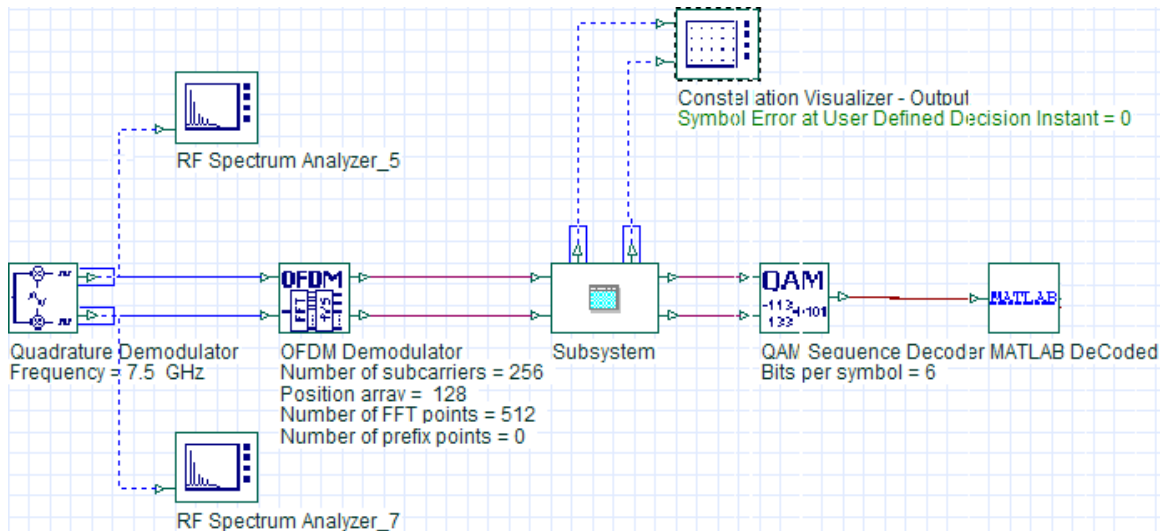
Figure 5.18: The receiver section of the RoF system

The first part is the quadrature demodulator which performs the analog demodulation for I and Q components, the OFDM demodulator is utilized to produce the digital signal from the OFDM signal received and the QAM Sequence decoder is used to convert the two parallel M-ary symbol sequences into

binary. The last part is the Matlab component which transports the binary sequence to Simulink for decoding the channel code and for the error calculations with respect to the original data sequence.

The quadrature demodulator is configured so as to compensate for and synchronize the phase and gain changes occurring in the received signal constellation, the configurations were made through trials and the least error readings were considered which are defined in the sections to follow.

For all the readings taken and the calculations in the following section, the Matlab generates a bit sequence of 5461 bits which are turbo coded with a coding rate of 1/3 and the resulting 16384 bits are forwarded to the Optisystem for transmission.

The analysis of the received data is done at the Matlab component (see Figure 5.18) and the BER calculations with respect to the SNR measured for the different fiber lengths in Table 5.4, is carried out. The plot of the BER at specific SNR for the number of decoding iterations is shown in Figure 5.19 for the 16-QAM scheme using 512 subcarrier OFDM.

Figure 5.19: A graph showing the 16-QAM scheme's BER at the specified decoding iterations for the given SNR

As it is visible from the graph, the BER worsens with the decrease in the SNR, for a specific decoding iteration. However, better BER can be expected for higher number of decoding iterations at relatively larger SNR values. The next graph, in Figure 5.20, shows the relation of the BER with the decoding iterations.

Figure 5.20: A graph showing 16-QAM scheme's BER for the specific decoding iteration with different fiber lengths

The graph shows the BER for the fiber lengths of 200km and 250km at the bottom because it is mostly zero from the first decoding iteration, while for the longer lengths of the fiber, the gradual decrease in BER is observable with the number of decoding iterations for the 16-QAM scheme employing 512 subcarrier OFDM signaling. The constellation diagram for the same signal is analysed from the constellation visualizer (see Figure 5.18) and the outputs for the different fiber lengths are listed in the set of graphs depicted in Figure 5.21 and Figure 5.22.
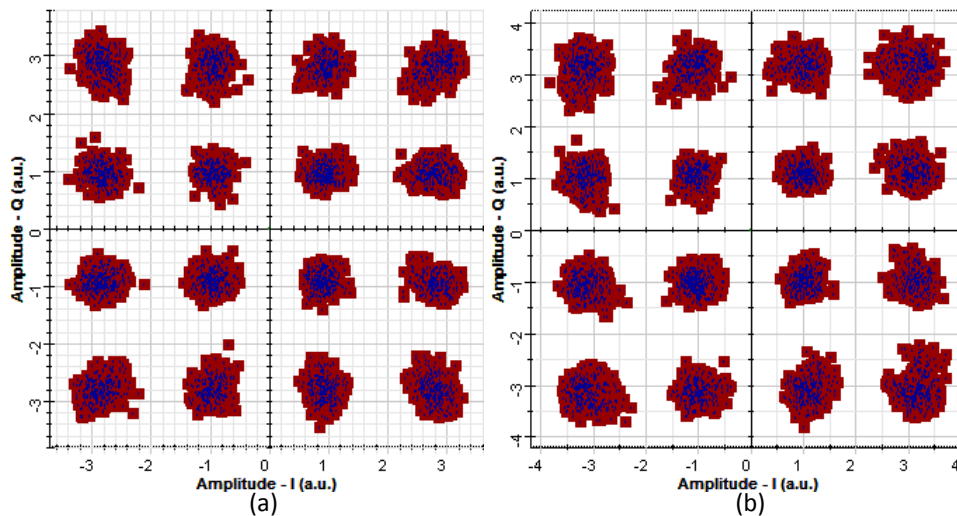
Figure 5.21:The signal constellations of the 16-QAM scheme at the receiver section for a fiber length of (a) 50 km and (b) 100 km

The red dots in the constellation diagram exhibit the signal while the blue dots depict the noise. The constellations for the longer fiber lengths are depicted in Figure 5.22.

Figure 5.22 The signal constellations of the 16-QAM scheme at the receiver section for a fiber length of (a) 200 km (b) 300 km and (c) 400 km

As we can see the constellation diagrams for the 50km and 100km length of fiber are fairly clear and one can distinguish between the different levels but the diagrams become distorted as the length of the fiber is increased as shown in Figure 5.22. The BER analysis for the 64-QAM scheme with 512 subcarrier OFDM signaling is presented next in the Figure 5.23 which shows the BER for the SNR values measured previously, listed in Table 5.4.
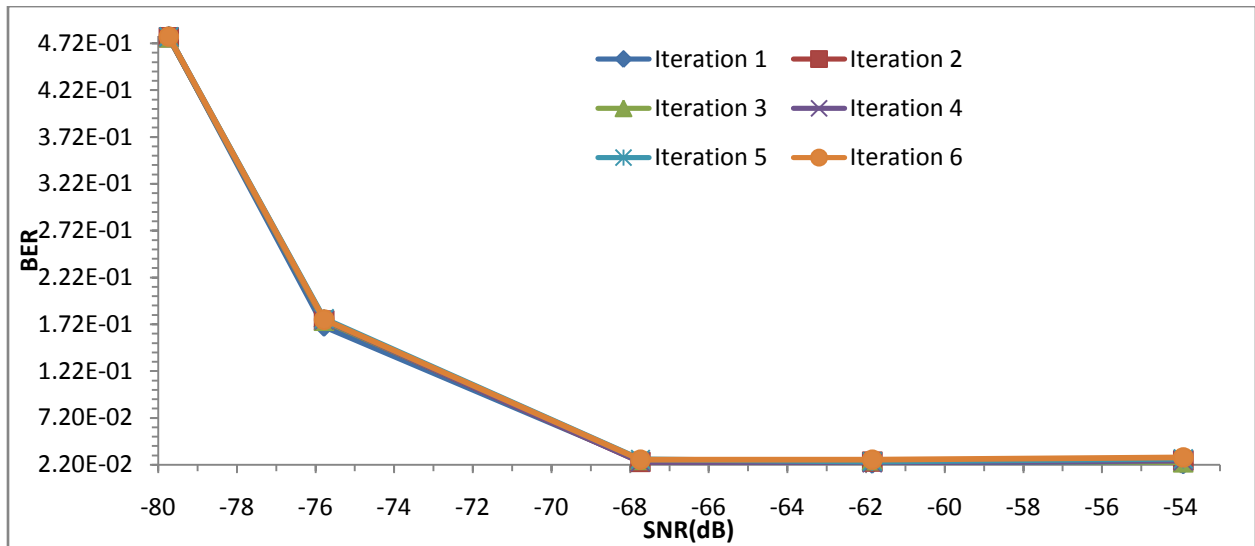
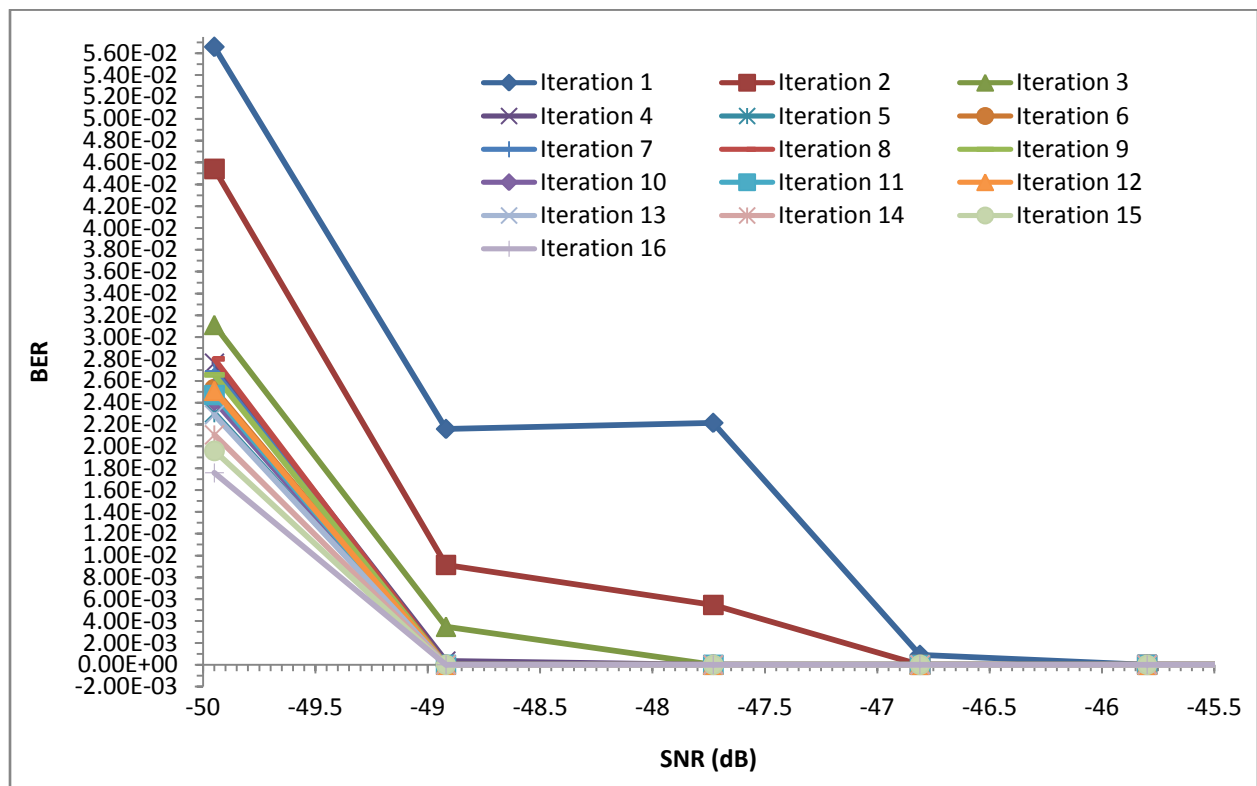**Figure 5.23: A graph showing the 64-QAM scheme's BER at the specified decoding iterations for the given SNR**

The graph defines the worsening BER with the decrement in SNR, however, the higher decoding iterations do not seem to affect the BER. The reason behind this shortcoming will be described by the analysis of Figure 5.25. To analyze the effect of the decoding iterations on the BER, the graph in Figure 5.24 is plotted for the different fiber lengths.
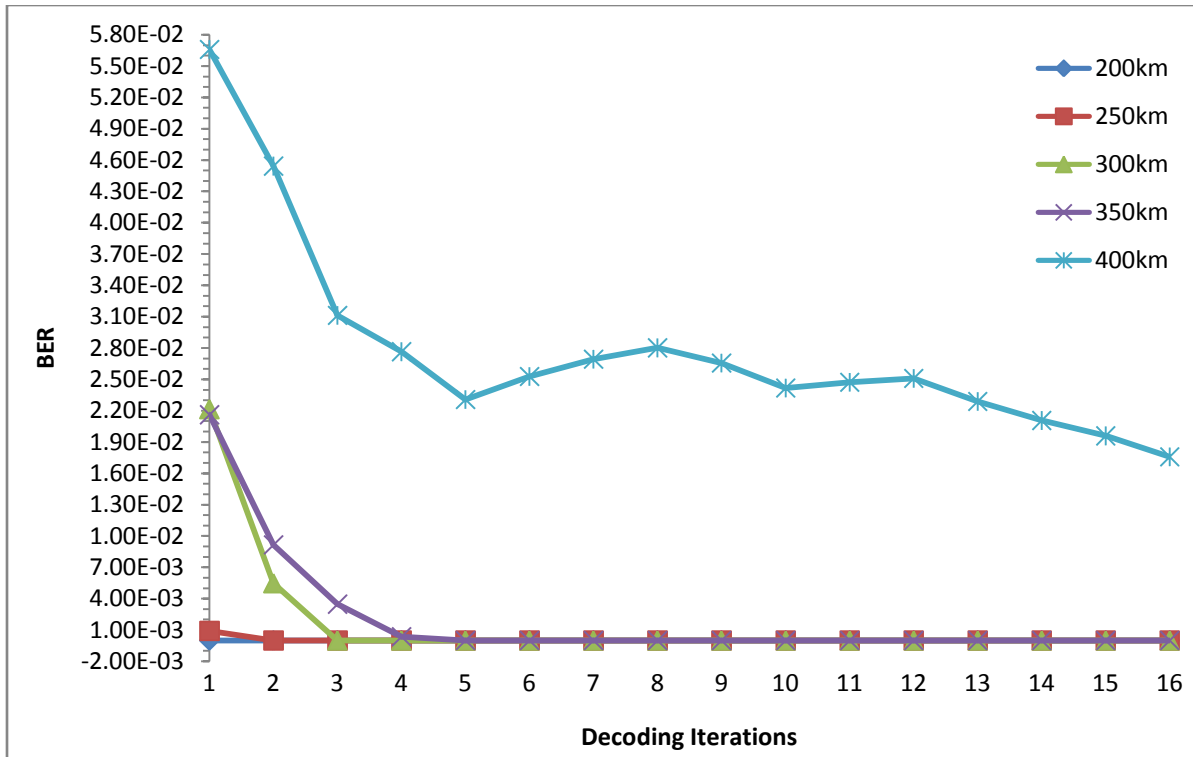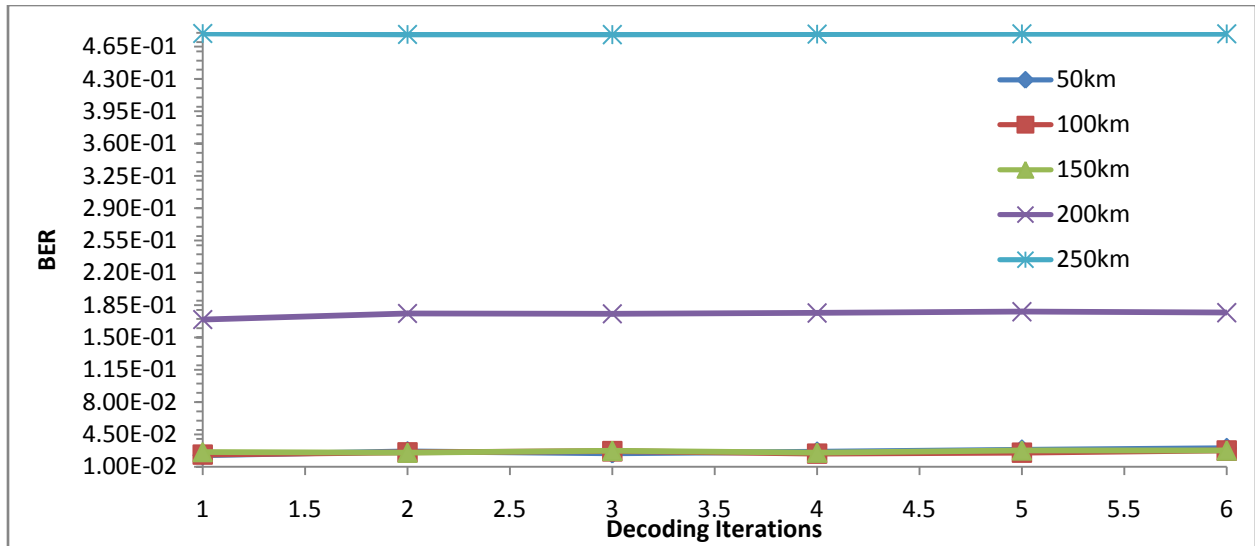
Figure 5.24: A graph showing 64-QAM scheme's BER for the specific decoding iteration with different fiber lengths

The decoding iterations were unable to decode beyond a negligible value, a possible reason to this shortcoming is considered as the number of bits per symbol are increased, the amount of information that goes into a symbol is also increased. Therefore, if a large amount of symbols are received in error, then the decoder is unable to rectify the data received in error. The same property is linked with the number of subcarriers, because a larger number of subcarriers provides a close packing of data bits, and more information is sent across the channel within one OFDM symbol. To understand the concept, the 64-QAM scheme is analyzed with a number of subcarriers and the graph is shown in Figure 5.25.
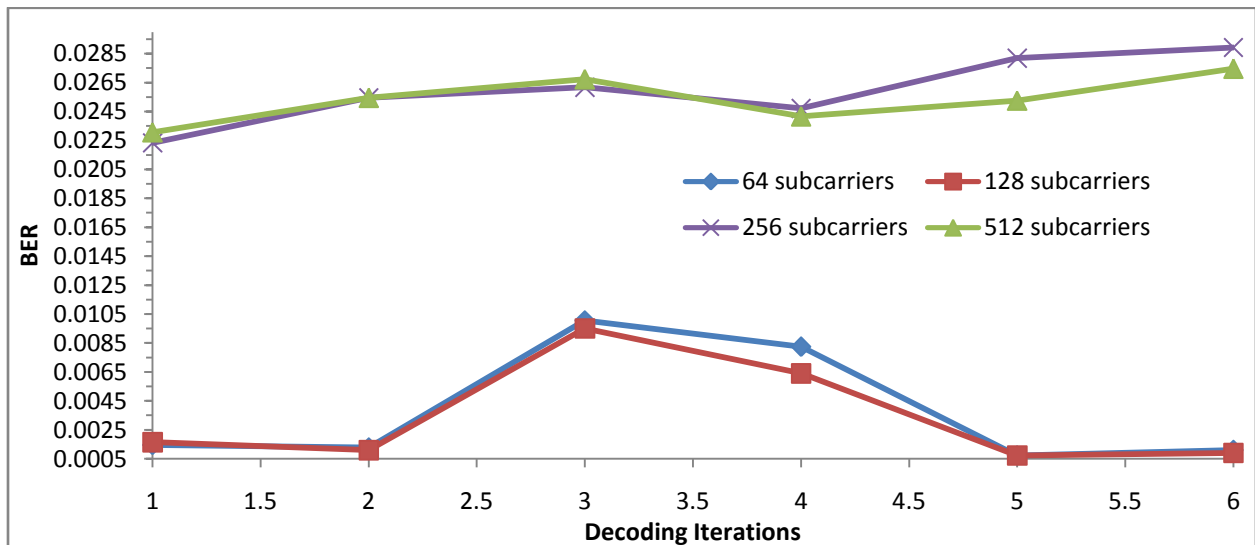
Figure 5.25: A graph showing 64-QAM scheme's BER for the specific decoding iteration with various number of subcarriers for a fiber length of 100km

As discussed above, the observable outcome from the graph also shows the larger subcarrier scheme having a BER relatively worse than the lower subcarrier schemes which somewhat describes the below

par performance of the decoder for the 64-QAM scheme. The constellation diagrams for the received 64-QAM signal are shown in the Figure 5.26
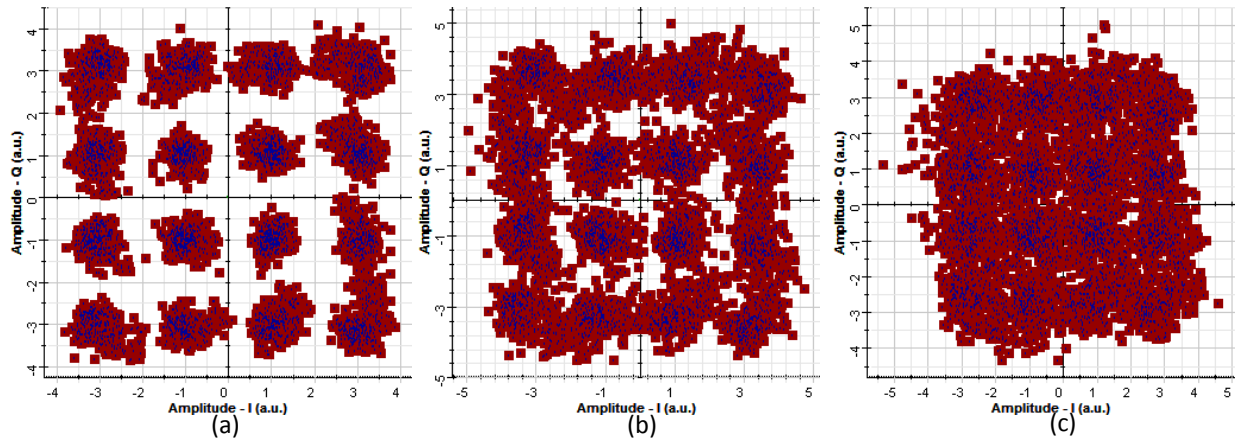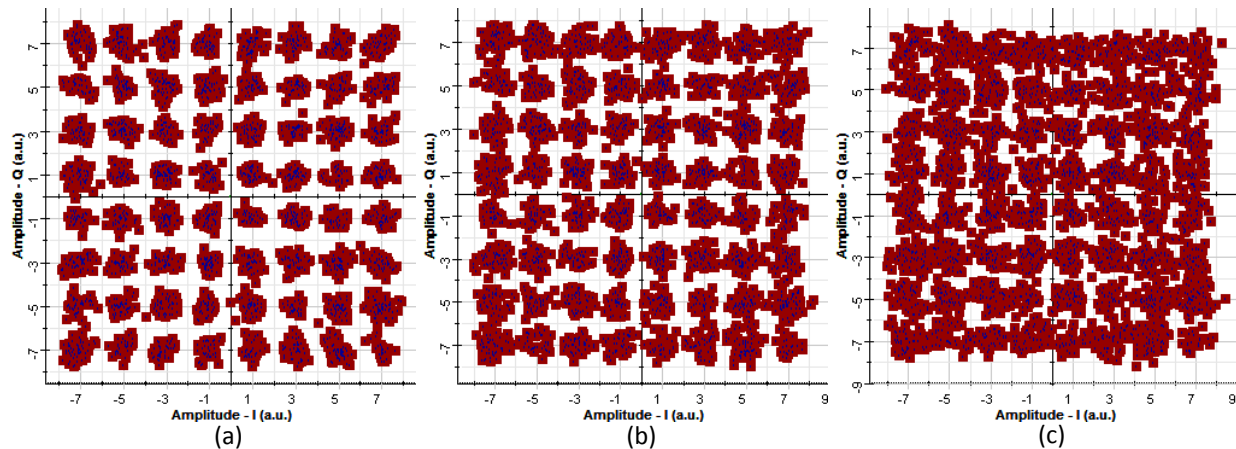

Figure 5.26: The signal constellations of the 64-QAM scheme at the receiver section for a fiber length of (a) 50 km (b) 100 km and (c) 150 km

The 64-QAM scheme uses 6 data bits per symbol and as we can observe from the constellation diagrams in Figure 5.26, that the symbols are placed close to each other and the distortion of the constellation diagram occurs for relatively shorter distances; if compared to the 16-QAM scheme.

For the 250km length of fiber the constellations get distorted up to the point where about half of the symbols are received in error. The signal constellations for the fiber lengths of 200km and 250km are displayed in Figure 5.27.
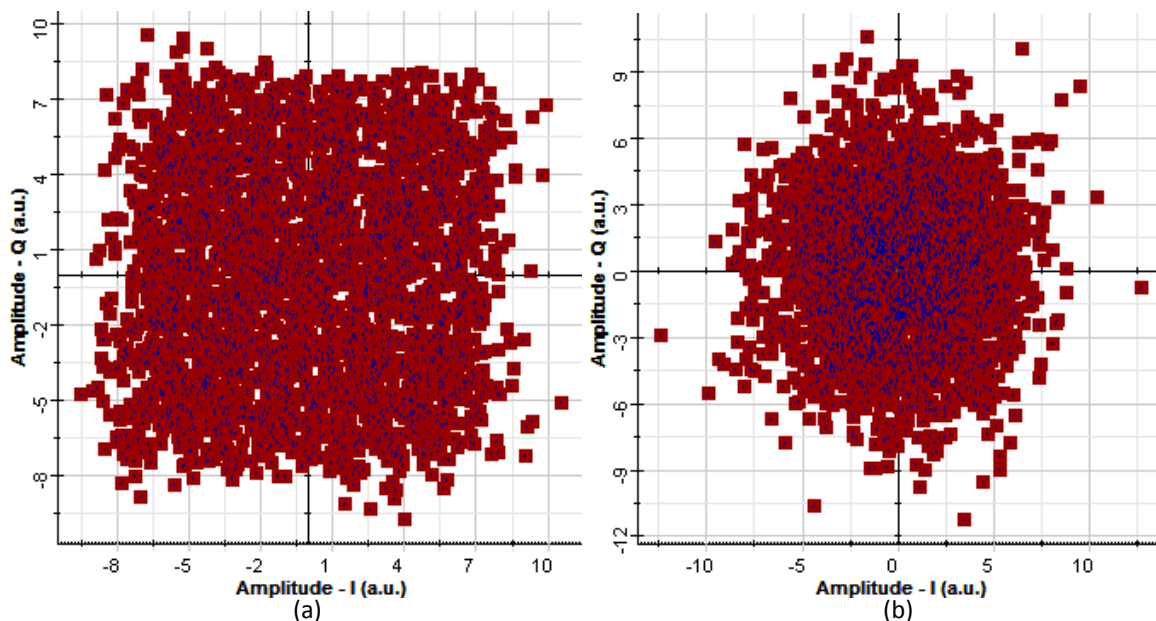
Figure 5.27: The signal constellations of the 64-QAM scheme at the receiver section for a fiber length of (a) 200 km and (b) 250 km

6   Conclusions and Future work

6.1   Conclusion

The Radio over Fiber technology is a valuable technology which provides the integration of wireless and optical communication platforms. With the recent introduction of high speed wireless broadband communications standards including 4G and LTE in Pakistan, the RoF technology can be implemented as a low-cost solution for extending the range of the wired communication networks to remote areas. With the efficiency of fiber optic links and the capability to transport data in excess of TB/s for long distances, the RoF provides a cost effective solution for multiple communication standards, which can share a single radio over fiber platform while keeping their data integrity intact.

This study of the radio over fiber system model provides an insight in the capabilities of the technology by simulating the results for different modulation formats i.e.16- and 64-QAM and for different optical fiber lengths extending up to 400km. The OFDM provides the advantage of parallel transmission with multiple subcarriers and is an integral part of the RoF technology. The integration with Matlab and Simulink platforms provides an expanded capability for the data processing and calculation, as the channel codec operations were carried out in the same domain for the study. The application of turbo codes provides a better error correction capability for the radio over fiber system with iterative decoding.

The simulations were carried out in the Optisystem, an optical simulator and the bit error rate calculations were carried out with Matlab. The signal constellations were verified for the correct phase matching at the receiver section of the RoF system model before the iterative decoding procedures were carried out. The transmission of 16-QAM signal on an OFDM signal with 512 subcarriers was successfully demonstrated for a 400km length of fiber and BER improvement of 10^{-1} was achieved for the received signal; with iterative decoding procedure.

The 64-QAM scheme was implemented for the 512 subcarriers OFDM signal, however a truthful decoding of the received sequence was not achieved because of the excess losses incurred due to the electro-optic conversion processes and the close packing of the information by the subcarriers.

Radio over Fiber is a technology that encompasses two large domains and therefore incessant improvements with ever increasing research are taking place. Some of the future studies relating to the given thesis can be implemented for a more robust and efficient system.

6.2   Future Work

This study provides the concept of the RoF technology along with a complete operational model for future research. Some of the future recommendations are presented here for a prospective boost to the given study.

- For a better understanding of the losses incurred during transmission, channel estimation techniques can be implemented with the help of Matlab integration which would allow for better channel coding and decoding.

- Application of a low cost system with multimode fibers is also a growing domain as the multimode fiber offers different modes for transmission with selectivity and it can perform reasonably well with low cost optical sources for e.g. VCSEL.

- Enhancements in the channel codes or replacements for e.g. Low density parity check (LDPC) codes can be implemented as many new standards of communication are being tested with it.

- Multiplexing techniques like WDM and DWDM can be utilized for increased bitrates for longer spans of fiber.

- The Matlab integration can be utilized further by an increased influence of the software on the complete RoF system. With Matlab, the data processing functions can be executed outside Optisystem therefore faster processing could be achieved. The study for the 64-QAM modulation scheme can be implemented and if required; enhanced with Matlab.

- The option of testing multiple wireless communications standards becomes possible with Matlab as the latest wireless standards are widely being tested and developed on Matlab also.

- Different optical sources, some of them already discussed in the study; can be tested with the studied model, for better transmission characteristics.

- Optisystem's compatibility with Agilent provides a helpful domain for the realization of real world RoF system.

- Cloud Radio Access Networks [9], and 60 GHz small cells [9] are some of the emerging concepts being explored for these next generation wireless systems, which have the potential to significantly impact the evolution of converged optical and wireless networks[9].

References

[1]   Beas, J., et al., *Millimeter-wave frequency radio over fiber systems: A survey.* Communications Surveys & Tutorials, IEEE, 2013. **15**(4): p. 1593-1619.

[2]   Wells, J., *Faster than fiber: The future of multi-G/s wireless.* Microwave Magazine, IEEE, 2009. **10**(3): p. 104-112.

[3]   Cisco. *Cisco Visual Networking Index: Forecast and Methodology, 2013–2018*. 2014 June 10,2014;   Available   from: http://www.cisco.com/c/en/us/solutions/collateral/service-provider/ip-ngn-ip-next-generation-network/white_paper_c11-481360.html.

[4]   Cisco. *Cisco Visual Networking Index: Global Mobile Data Traffic Forecast Update, 2013–2018*. 2014   February   5,   2014;   Available   from: http://www.cisco.com/c/en/us/solutions/collateral/service-provider/visual-networking-index-vni/white_paper_c11-520862.html.

[5]   ERICSSON. *Ericsson Mobility Report, June 2014*. 2014 June 2014; Available from: http://www.ericsson.com/res/docs/2014/ericsson-mobility-report-june-2014.pdf.

[6]   Gomes, N.J., P.P. Monteiro, and A. Gameiro, *Next generation wireless communications using radio over fiber*. First ed. 2012: John Wiley & Sons.

[7]   Attar, A., H. Li, and V.C. Leung, *Green last mile: how fiber-connected massively distributed antenna systems can save energy.* Wireless Communications, IEEE, 2011. **18**(5): p. 66-74.

[8]   Oliveira, J.M.B.d., *Receiver Design for Nonlinearly Distorted OFDM Signals: Applications in Radio-over-Fiber Systems.*, in *Department of Electrotechnical and Computers Engineering*. 2011, University of Porto: Portugal.

[9]   Novak, D. and R. Waterhouse, *Advanced radio over fiber network technologies.* Optics express, 2013. **21**(19): p. 23001-23006.

[10]   Ng'oma, A., *Radio-over-Fibre Technology for Broadband Wireless Communication Systems.*, in *Electrical Engineering*. 2005, Eindhoven University of Technology: Netherlands.

[11]   Pang, X., et al., *25 Gbit/s QPSK hybrid fiber-wireless transmission in the W-band (75–110 GHz) with remote antenna unit for in-building wireless networks.* Photonics Journal, IEEE, 2012. **4**(3): p. 691-698.

[12]   Brendel, F., *Millimeter-Wave Radio-over-Fiber Links based on Mode-Locked Laser Diodes*. Vol. 68. 2013: KIT Scientific Publishing.

[13]   Lim, C., et al., *Fiber-wireless networks and subsystem technologies.* Lightwave Technology, Journal of, 2010. **28**(4): p. 390-405.

[14]   Yu, J., X. Li, and N. Chi, *Faster than fiber: over 100-Gb/s signal delivery in fiber wireless integration system.* Optics express, 2013. **21**(19): p. 22885-22904.

[15]   Iezekiel, S., *Microwave photonics: devices and applications*. Vol. 3. 2009: John Wiley & Sons.

[16]   Cox, C.H., *Analog optical links: theory and practice*. 2006: Cambridge University Press.

[17]   Koonen, A.M., et al. *Perspectives of radio-over-fiber technologies*. in *Optical Fiber Communication Conference*. 2008. Optical Society of America.

[18]   Chang, W.S., *RF photonic technology in optical fiber links*. 2002: Cambridge University Press.

[19]   Huang, H., et al. *100-Gbit/s amplitude and phase modulation characterization of a single-drive, Low-Vπ polymer mach-zehnder modulator*. in *Optical Fiber Communication Conference*. 2012. Optical Society of America.

[20]   Wake, D., A. Nkansah, and N.J. Gomes, *Radio over fiber link design for next generation wireless systems.* Lightwave Technology, Journal of, 2010. **28**(16): p. 2456-2464.

[21]   Larrode, M.G., et al. *Transparent transport of wireless communication signals in radio-over-fibre systems*. in *Proc. Eur. Conf. Netw. Opt. Commun*. 2005.

[22] Al-Raweshidy, H. and S. Komaki, *Radio over fiber technologies for mobile communications networks*. 2002: Artech House.

[23] Fabbri, M. and P. Faccin. *Radio over fiber technologies and systems: New opportunities*. in *Transparent Optical Networks, 2007. ICTON'07. 9th International Conference on*. 2007. IEEE.

[24] Bello, P.A., *Selective fading limitations of the Kathryn modem.* 1967.

[25] Powers, E. and M. Zimmermann. *A digital implementation of a multichannel data modem*. in *Proc. IEEE Int. Conf. Commun*. 1968.

[26] Chang, R.W., *Synthesis of Band-Limited Orthogonal Signals for Multichannel Data Transmission.* Bell System Technical Journal, 1966. **45**(10): p. 1775-1796.

[27] Salz, J. and S. Weinstein. *Fourier transform communication system*. in *Proceedings of the first ACM symposium on Problems in the optimization of data communications systems*. 1969. ACM.

[28] Weinstein, S. and P. Ebert, *Data transmission by frequency-division multiplexing using the discrete Fourier transform.* Communication Technology, IEEE Transactions on, 1971. **19**(5): p. 628-634.

[29] Hirosaki, B., *An analysis of automatic equalizers for orthogonally multiplexed QAM systems.* Communications, IEEE Transactions on, 1980. **28**(1): p. 73-83.

[30] Peled, A. and A. Ruiz. *Frequency domain data transmission using reduced computational complexity algorithms*. in *Acoustics, Speech, and Signal Processing, IEEE International Conference on ICASSP'80.* 1980. IEEE.

[31] Cimini, L.J., *Analysis and simulation of a digital mobile channel using orthogonal frequency division multiplexing.* Communications, IEEE Transactions on, 1985. **33**(7): p. 665-675.

[32] Lassalle, R. and M. Alard, *Principles of modulation and channel coding for digital broadcasting for mobile receivers.* EBU Tech. Rev, 1987. **224**: p. 168-190.

[33] Armstrong, J., *OFDM for optical communications.* Journal of lightwave technology, 2009. **27**(3): p. 189-204.

[34] Koffman, I. and V. Roman, *Broadband wireless access solutions based on OFDM access in IEEE 802.16.* Communications Magazine, IEEE, 2002. **40**(4): p. 96-103.

[35] Reimers, U., *Digital video broadcasting.* Communications Magazine, IEEE, 1998. **36**(6): p. 104-110.

[36] Keller, T. and L. Hanzo, *Adaptive multicarrier modulation: A convenient framework for time-frequency processing in wireless communications.* Proceedings of the IEEE, 2000. **88**(5): p. 611-640.

[37] Zou, W.Y. and Y. Wu, *COFDM: An overview.* Broadcasting, IEEE Transactions on, 1995. **41**(1): p. 1-8.

[38] CIMINI JR, L.J. and Y.G. LI. *Orthogonal frequency division multiplexing for wireless channels*. in *IEEE Globecom*. 1998.

[39] Bahai, A.R., B.R. Saltzberg, and M. Ergen, *Multi-carrier digital communications: theory and applications of OFDM*. 2004: Springer.

[40] Wei, X., H. Guijun, and D. Qing, *Application of Turbo codes in optical OFDM multimode fiber communication system.* Optics Communications, 2008. **281**(5): p. 1118-1122.

[41] Shieh, W. and I. Djordjevic, *OFDM for optical communications*. 2009: Academic Press.

[42] Haykins, S., *Digital communication*. Vol. 11. 2010: Willey India.

[43] Valenti, M.C. and J. Sun, *Turbo codes.* Handbook of RF and Wireless Technologies, 2004: p. 375-400.

[44] SHANNON, C., *A Mathematical Theory of Communication.* 1948.

[45] Hokfelt, J., *On the design of turbo codes*. 2000: Lund University.

[46]   Berrou, C., A. Glavieux, and P. Thitimajshima. *Near Shannon limit error-correcting coding and decoding: Turbo-codes. 1*. in *Communications, 1993. ICC '93 Geneva. Technical Program, Conference Record, IEEE International Conference on*. 1993.

[47]   Mathys, P., *Theory and Practice of Error Control Codes*. 2003: University of Colorado.

[48]   Waggener, B., *Pulse code modulation techniques*. 1995: Springer.

[49]   Peterson, W.W. and E.J. Weldon, *Error-correcting codes*. 1972: MIT press.

[50]   Hagenauer, J., *Rate-compatible punctured convolutional codes (RCPC codes) and their applications.* Communications, IEEE Transactions on, 1988. **36**(4): p. 389-400.

[51]   Heegard, C. and S.B. Wicker, *Turbo coding*. 1999: Springer.

[52]   Goldsmith, A., *Wireless communications*. 2005: Cambridge university press.

[53]   Reichenbach, H., *The theory of probability*. 1971: Univ of California Press.

[54]   Berrou, C., et al. *An overview of turbo codes and their applications*. in *Wireless Technology, 2005. The European Conference on*. 2005. IEEE.

[55]   Zizheng, C., et al., *Direct-Detection Optical OFDM Transmission System Without Frequency Guard Band.* Photonics Technology Letters, IEEE, 2010. **22**(11): p. 736-738.

[56]   Bhatia, K., T. Kamal, and R. Kaler, *An adaptive compensation scheme-based coded direct detection optical–orthogonal frequency division multiplex (OFDM) system.* Computers & Electrical Engineering, 2012. **38**(6): p. 1573-1578.

[57]   Dimmler, W., et al., *Method and apparatus to compensate for atmospheric effects and target motion in laser communication system*. 2001, Google Patents.

[58]   Yi, C., et al., *On turbo code decoder performance in optical-fiber communication systems with dominating ASE noise.* Lightwave Technology, Journal of, 2003. **21**(3): p. 727-734.

[59]   Janz, S., J. Čtyroký, and S. Tanev, *Frontiers in Planar Lightwave Circuit Technology*. 2006: Springer.

[60]   Optiwave. 2014 [cited 2014; Available from: www.optiwave.com.